CHALMERS

Preventing the growth of barnacles by using ultrasonic sound

Master of Science Thesis in the Master's Programme in Sound and Vibration

DIANA GÓMEZ OLMEDILLA

Department of Civil and Environmental Engineering
Division of Applied Acoustics
Vibroacoustics Research Group
CHALMERS UNIVERSITY OF TECHNOLOGY
Göteborg, Sweden 2012

Master's Thesis 2012:06

MASTER'S THESIS 2012:06

Preventing the growth of barnacles by using ultrasonic sound

Master of Science Thesis in the Master's Programme in Sound and Vibration

Diana Gómez Olmedilla

Department of Civil and Environmental Engineering

Division of Applied Acoustics

Vibroacoustics Group

CHALMERS UNIVERSITY OF TECHNOLOGY

VOLVO PENTA AB.

Göteborg, Sweden 2012

Preventing the growth of barnacles by using ultrasound sound

Master of Science Thesis in the Master's Programme in Sound and Vibration
DIANA GOMEZ OLMEDILLA

Department of Civil and Environmental Engineering
Division of Division of *Applied Acoustics*
Vibroacoustics Research Group
Chalmers University of Technology
SE-412 96 Göteborg
Sweden
Telephone: + 46 (0)31-772 1000

Cover:
Picture by Kim Wroth, taken on a drainage ditch in Clear Lake, TX. USA, 2011.

Reproservice, Department of Civil and Environmental Engineering Göteborg, Sweden
2012

Preventing the growth of barnacles by using ultrasonic sound

Diana Gómez Olmedilla

Department of Civil and Environmental Engineering

Division of Applied Acoustics

Vibroacoustics Group

Chalmers University of Technology

Abstract

Master thesis: Preventing the growth of barnacles by using ultrasonic sound

Biofouling is produced by sessile organisms that attach to the hull of the ship affecting boat's hydrodynamic resistance and weight. Therefore, higher fuel consumption is required to keep fast cruise speed and consequently high economical periodic investment in hauling out & cleaning. This effect has being commonly prevented by using special coatings on the hull surface.

This master thesis has been carried out in cooperation with Volvo Penta AB and its goal is the evaluation of an alternative approach for antifouling purposes on the hull on the boats. The method is based on emitting signals within the ultrasounds range through the hull towards the water so as to create disturbances in the water nearby the submerged part of the boat, aiming to prevent barnacles from settling down on the hull's surface. In order to create the optimum signal the following factors are considered: organisms attachment preferences, material's coincidence radiation frequency and transducer resonance. For that purpose, a preliminary study of the specific specie of barnacle predominant in the west coast of Sweden - balanus improvisus- takes place; secondly, numerical analysis based on the Thick Plates Theory – Mindlin models - are carried out to observe the radiation pattern of an equivalent system to the ship hull; finally observance of the transducer performance.

The biological experiments carried out to examine the barnacles behavioural response towards generated sounds confirm that the existence of the sound affects their attachment preferences. On the other hand, radiation measurements on a hanged aluminium plate took place to be compared with the numerical models for infinite plates, and show that the transducer resonance has bigger influence in the transmitted energy than the materials resonances.

Future work should include radiation measurements with water load on one side or the inclusion of damping on the plate to adequate the plate response to the numerical models. Besides, more biological measurements should be carried out to ensure the results. Finally the conclusions regarding transmission at the transducer resonance should be taken into account to readjust the frequency range of the emitted signal in order to improve it.

Master of Science in Sound and Vibration
Institutionen för bygg- och miljöteknik
Chalmers tekniska högskola

Contents

1 Introduction

The goal of this project is to evaluate a technique to prevent sessile organisms from getting attached to the hull of the ship, phenomena known as biofouling. The approach is based on the transmission of ultrasounds through the boat's hull towards the water. The applied signal may create disturbances in the water nearby the submerged part of the boat, which may result in changes in the organisms' attachment preferences.

Biofouling affects the hydrodynamic resistance and total boat weight. Therefore, higher fuel consumption is required to counteract lower cruise speed. Additionally, fouling leads to high economical periodic investment in hauling out & cleaning.

The fouling phases are as follows: creation of micro-biological film, attachment of macroscopic fouling organisms – larvae form (prevent this point!) and their growth into the mature forms. Affected by the roughness of the surface (the harder and flatter, the better) also appealed to light colours, previous studies show that it could be possible to create a tide / current fast enough to avoid their attachment (range 3 to 6.5 km/h (1.6 to 3 knots), as stated in *Understanding Marine Fouling and Assessing Antifouling Approaches* [1].

Nowadays, regarding chemical antifouling approaches, new policies about the use of tributyl tin (TBT) and copper- based paintings have been established worldwide. For that reason the chemical industry has developed new paintings, like copolymer paints (SPC), based on the water hydrolysis phenomena, and fouling release coatings (FRC), based on polymers- silicon solutions. Also, other mechanisms based on electric and sound fields are being considered.

Key words: ultrasound, antifouling, Mindlin, underwater propagation.

1.1 Chapters review

This thesis deals with the transmission of ultrasounds through the hull as an alternative to the use of chemical coatings. Hence, in order to create the optimum signal the following factors are considered: organisms attachment preferences, material's coincidence radiation frequency and transducer resonance.

For that purpose, a preliminary study of the specific specie of barnacle predominant in the west coast of Sweden - balanus improvisus- takes place in chapter 2, including life cycle and specie characteristics.

Chapter 3 deals with the waves that are propagated through the material in accordance with different frequency ranges. This analysis has been used to observe the radiation pattern of plates that simulate the mechanical characteristics of the common hull constructions with - without water load. So as to examine sound transmission a review of the Thin Plates theory for medium frequencies takes place at first instance and it leads to the study of the Thick Plates theory, more appropriate in the situation of wavelengths comparable to the material thickness. This way, particle displacement and velocity can be calculated to obtain the radiated power over frequency, applicable in the situations of different fluid load on one side of the plate - air on the other side. Besides, examination on environmental impact on ultrasounds emission takes place regarding noise induced in the sea and possibility of bubbles implosion.

So as to check adaptation of the theoretical studies to reality, both biological and radiation measurements have been carried out. To this effect, Chapter 4 summarizes the design of aquariums, in which larvae were placed; selection of suitable aluminium plates for the radiation measurements; and experiments set up including all the necessary acquisition – processing equipment.

Finally, chapters 5 and 6 show collected results and conclusions. Regarding biological experiments, more measurements should be done so as to ensure enough statistical data as well as getting feasible results; on the radiation measurements, improvements in the procedure should include water load or at least added damping to the plate to adequate the real material with the infinite plate models.

2 Barnacles and life cycle

Sessile organisms within the maxillopoda family can be subdivided in different orders. One of these orders is the cirripeds which can therefore be subdivided between acrothoracica & thoracica class. The last class includes the suborders of goose and acorn barnacles. Acorn barnacles (i.e. balanus) are characterized by having soft body inside a conical wall formed by calcareous plates glued together. Two of those plates can be moved, creating an opening (called operculum) to let the barnacle leg (cirri) capture suspended plankton. The next sections cover a deeper look into the organisms' life cycle based on seven nauplius stages: fertilization of an egg, growth in size and storage of food reserves; cyprid phase in which the animal consumes the food reserves while looking for a suitable surface to get attached and start metamorphosis. From that stage the organism will remain on that surface until its death and feed from water nutrients, fulfilling juvenile – adult barnacle stages, this cycle can be seen in figure 2.

2.1 Larvae & nauplius stage

Although barnacles are hermaphrodites, their survival is based on cross- reproduction. This fact explains their tendency in populating the same areas for reproduction purposes. The process is based on the female deploying the eggs that are fertilized by the male character leading to the first larvae stage, known as nauplius. Nauplius has 3 pairs of cephalic limbs aimed for swimming and feeding purposes, in the case of cirripede type, it has horns with perforated tips and secretory cells around the top of the head (unknown funcionality). At this phase the nauplius stores lipids on its physiognomy.

As explained in *Factors influencing attachment fouling* [2], approximately two weeks after eggs fertilization (when accomplished "6^{th} nauplius stage") the larva suffers metamorphosis becoming a swimming cyprid larva: it swims with dorsal/ attaching surface upwards, being sensitive to light due to a possible negative phototropic response, which explains why they are usually found in warm but dark areas. At this stage, the organism begins seeking for a proper surface to settle down: the preferred surfaces may contain slim films with detritus & micro organisms. Given that the organism survival is based on food reserves, this stage has to be accomplished in a limited period of time, as explained by *Matz Berggren* [3].

Figure 1 shows the physiognomy of the nauplius while figure 2 summarises the whole balanus life cycle

Figure 1 Microscope caption of a balanus improvisus cyprid, represented in *Factors influencing attachment fouling* [2]. According to *Matz Berggren* [3], the dimensions of the balanus improvisus cyprid are 200 X 700 µm, approximately.

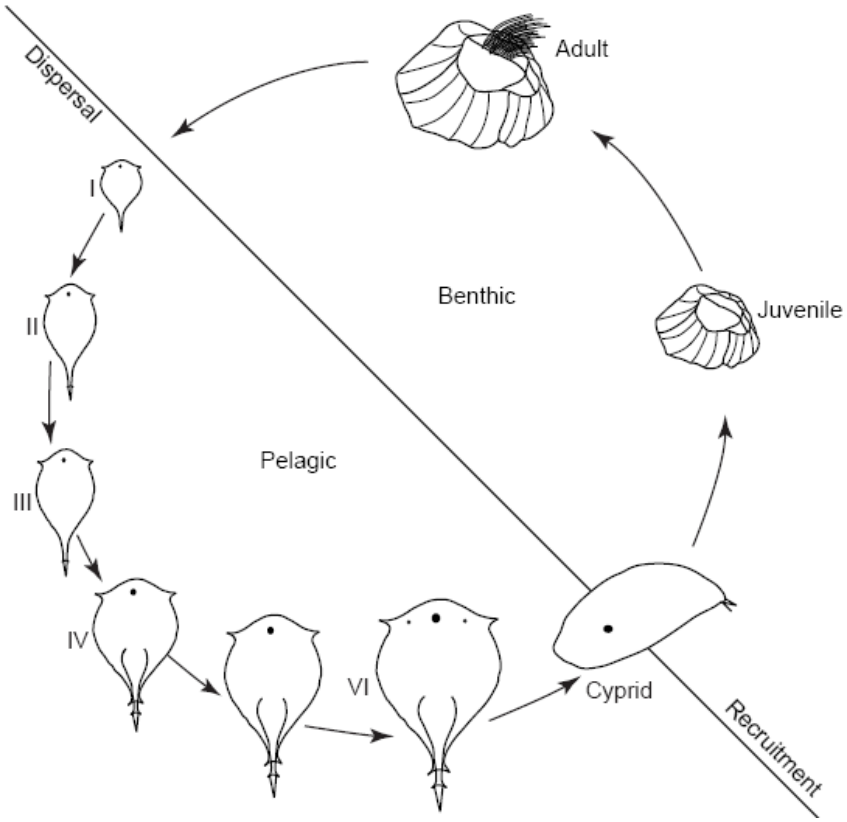

Figure 2. Complete balanus life cycle. Anticlockwise direction, from dispersal to recruitment the six nauplii stages can be seen. Nauplius evolution lead to cyprid – juvenile and finally adult life

In *Underwater adhesion: the barnacle way* [4], a complete analysis of the larvae growth can be reviewed. This article states that once concluded the nauplii stages, at the cyprid stage the animal has two parallel antennas with the features shown in the figure 3:

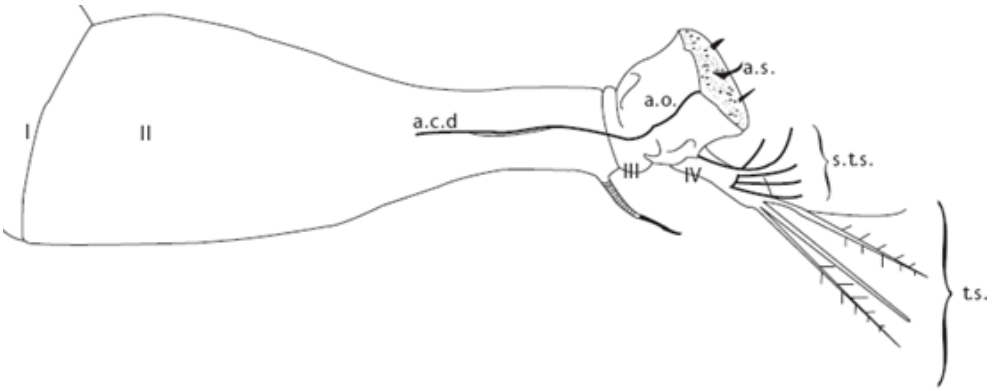

Figure 3 Sketch of the cyprid's antenna [4].

Where:

a.c.d is the axial cement duct which is connected to the attaching organ (**a.o**.) and ends in the attaching sensory cells (**a.s**). On the other side, the areas called **s.t.s** and **t.s** correspond to the subterminal and terminal setae, terminology according to *Lidita khandeparker & Arga Chandrashekhar* [4].

The function of the sensory cells is to evaluate the suitability of the surface, by secreting a temporal cement substance with the first antenna and then pulling from the cement to check the attachment endurance. At this stage, the cyprids can be self-detached in order to re- allocate closer to other barnacles for reproduction purposes, fact explained by *Matz Berggren* [3]. Once the permanent cement is secreted detachment cannot take place.

So as to produce the cement, the cyprid have ovoid glands that secrete phenolic compounds and phenolase enzyme (proteins), organisms' physiognomy and process explained in detail by *Underwater Adhesion, the barnacle way* [4]. Each larvae antenna contains 20 glands with the following features as seen in figure 4:

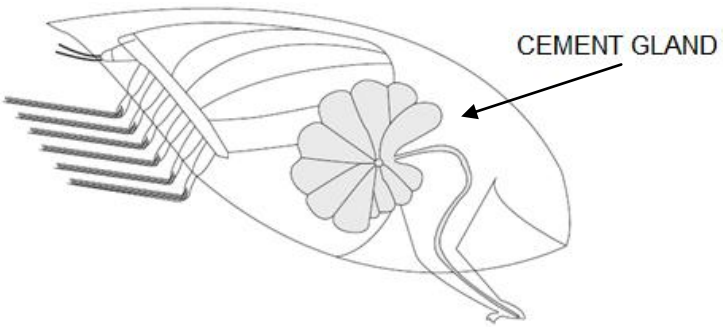

Figure 4. Cyprid physiognomy. The cement glands characteristics are: thickness 60 – 90 µm; length 150 µm and volume when full approximately 470 μm^3 [4]

They secrete the cement by exocytosis [1]: the doses are controlled by catecholaminergic neurons. The cement is made from proteins that are water – soluble, but they are secreted with enzymes that oxidize and make them insoluble (chemical solutions such as hydrolyzing adhesive polymers, oil them).

[1] Chemical process in which the vesicles placed in cytoplasm blend with the plasma membrane.

The amount of calcium secreted by the cement glands depends on the surface's Young Modulus [E]. The moment that the animal perceives that the surface is suitable for settling down, it secretes epoxy-like permanent cement and starts the change to juvenile barnacle.

The first step of the metamorphosis is the transformation of the cyprid's swimming legs into adult's feeding limbs and the body rotation. Besides, the second antenna is lost during metamorphosis. Moreover the larva's medium eye (the larvae posses three ayes aligned) turns into adult's photoreceptor. At the same time, the lateral parts of this medium eye displace towards both sides inside the moving plates to be able to detect predators in shadows (and thus close the top plates).

Finally, at cyprid stage, inside the cytoplasm[2] of the cement cells there are inner channels connected to larger extra cement ducts, which are lost while metamorphosis and no longer exist in the calcareous base[3]

[2] Cell's part surrounded by a membrane, it does not include the nucleus.

[3] The calcareous base forms the adult barnacle's outdoor plates.

The final metamorphosis stage and the settle down process can be observed in figure 5.

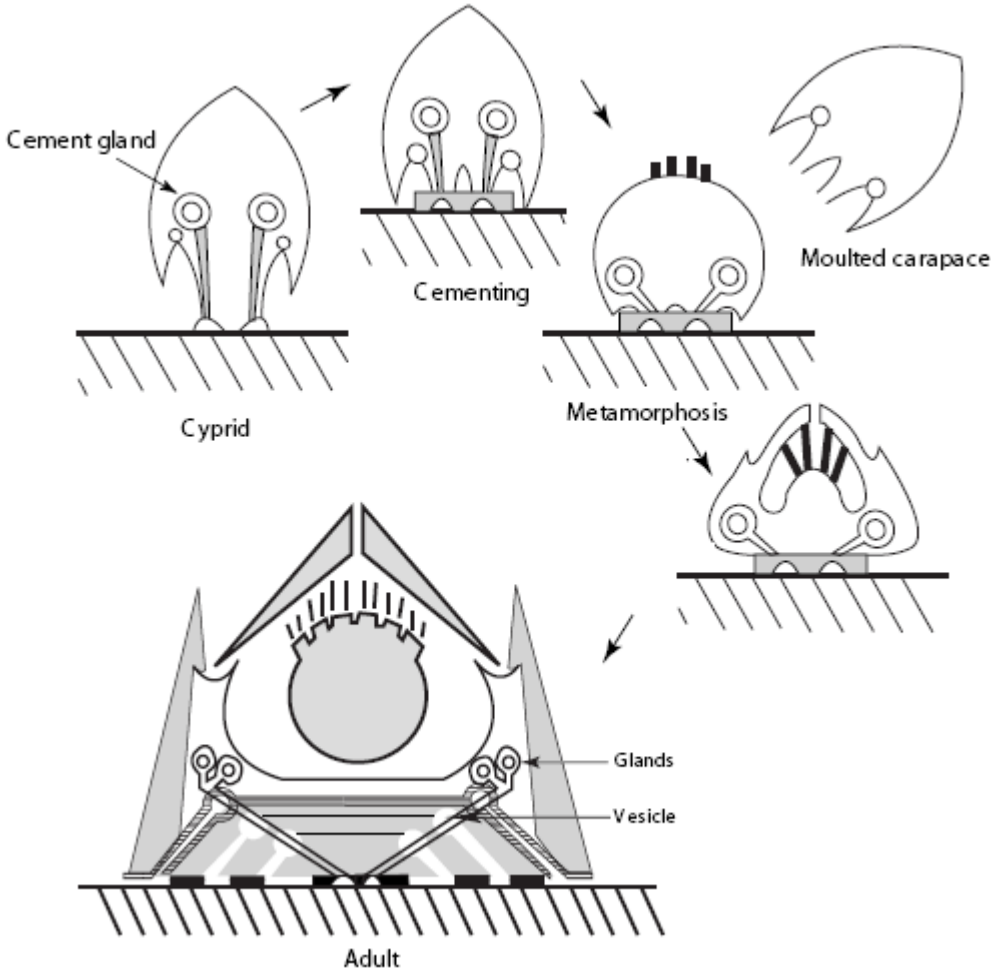

Figure 5. Development from cyprid to adult barnacle, *Underwater adhesion: the barnacle* way [4].

2.2 Adult barnacle physical features

The final barnacle growing stage is the adult barnacle. Its physiology has been studied by *Karl Tate* [5] and can be observed in figure 6,

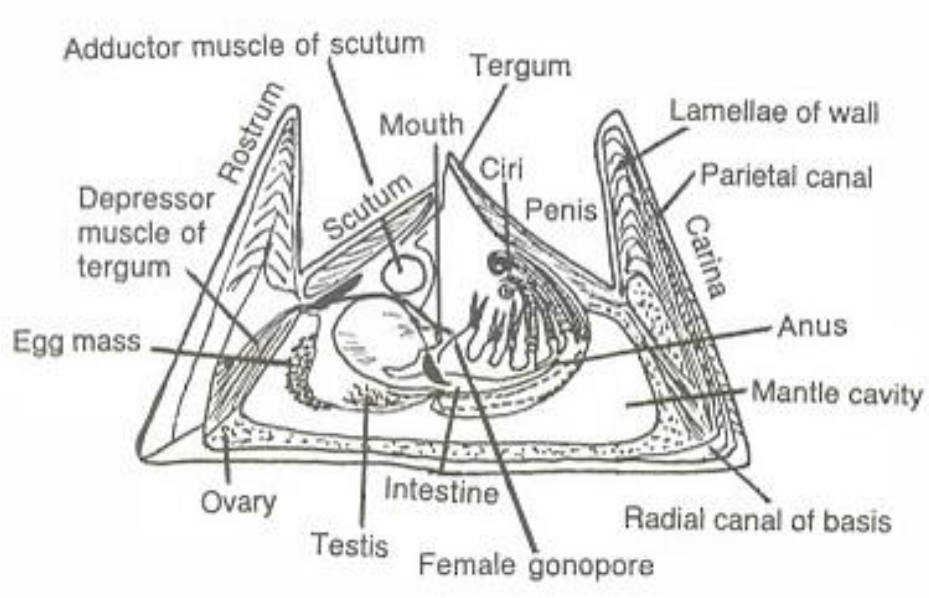

Figure 6. Adult barnacle's inner organs, further explanations by *Karl Tate* [5].

Basically, the adult barnacle is able to control the movement of top plates due to transverse abductor and discrete retractor muscles. Inside the calcareous plates, the animal contains blood and water circulation in & out of the mantle takes place. In the previous figure 6, basic sketch of the adult balanus can be reviewed.

2.3 Other considerations on barnacles

As explained before, the critical growth stage comes with the settlement phase, and due to the size of the organisms and its resistance towards environmental conditions, these organisms proceed with surface seeking in quiet waters – thus, moored objects mainly, as explained by *Factors influencing the attachment and adherence of fouling organims* [2]. Another study, done by *Visscher* [6] reinforces this theory stating that the maximum registered velocity – water flow that balanus improvisus can cope with while attachment is about 0.5 knot. This article also remarks that so as to remove existing organisms up to 16 days old, water flow of 4 knot had to be applied. On the other hand, it refers to an experimental try with air bubbles that successfully worked but imply the use of large quantities of air.

In accordance with *Simone Dürr & Jeremy C. Thomason* [7], water currents annoyance varies within the different barnacles species, so that large mussels and so on can deal with faster water velocities than balanus.

Consequently, current flows affect the life cycle:

1. On one hand, introducing annoyance produced while attachment.
2. Whereas on the other hand, increasing nutrients flow leads to an increase of food surrounding the animal. Moreover, a consequence of water renewal is that a bigger amount of metabolic waste is removed, thus benefitting the culture growth.

According to *Matz Berggren* [3], this fact is explained given that those organisms (algae, microorganisms...) cover the surface with substances that make balanus cyprid slip, preventing their attachment.

In west coast of Sweden there exist considerable populations of balanus improvisus, for other locations, dominant species are pointed by *European Network of invasive species* (barnacles' distribution in different seashores) [8].

3 Waves propagation & frequency range

The beginning of this chapter reviews the Thin Plates Theory, common approach used for low – medium frequencies at which bending waves are propagated. The Thin Plates Theory neglects torsion and inertia moment, which are phenomena that are noticeable at frequencies where the wavelength is comparable to the thickness of the material (high frequency). Given that thesis contemplates ultrasonic frequency range, the numerical models based on the Thin Plates Theory are not adequate any longer, and thus the analysis is carried out applying the Thick Plates Theory instead of the Thin Plates Theory.

3.1 Case study overview & boundary conditions

The observed plates performing as the hull materials are considered to be isotropic, infinite plates with no displacement or torque moments at the sides. For the numerical approach infinite plates have been considered, the results can be applied to finite plates at high frequencies given the next statements:

1. Existence of high modal density near and above coincidence frequency, as explained in *Sound, Structures and Their Interaction* [9].
2. Neglect edges reflections provided the following requirements are fulfilled: enough damping on the structure so as to dissipate energy and plate dimensions big enough to contain many wavelengths.

Note that for the construction of safe boats, the hull's thickness varies around 1 inch (2.54 cm) as pointed by institutions such as *American Boat & Yacht Council* [10], as this thickness varies from different types of boats and the tendency is in using less material, this study contemplates theoretical hull thickness of 1 cm.

The purpose of this case study is to apply a harmonic point force from the inner side of the hull to create a wave pattern outside the hull (water side) aiming to induce particle velocity in a range of few centimetres towards the water. Causing a small disturbance that may be uncomfortable for cyprids to settle down. For the feasibility of the analysis, instead of observing a boat's hull, plates are considered to be a reasonable simpler model;

In the analysis of harmonic point force applied at the origin and in the direction of the positive displacement, the response relies on the distance from that point leading to an axisymmetric behaviour – in the plane of the plate; hence for practical purposes the phenomena can be analyzed applying cylindrical coordinates. The translation from Cartesian coordinates to cylindrical coordinates for this case study is shown in figure 7.

h is the plate thickness (1 cm).

Cylindrical coordinates: $z = R\cos(\theta)$, $r = Rsin(\theta)$

Being (R, θ) represented in the following figure 7:

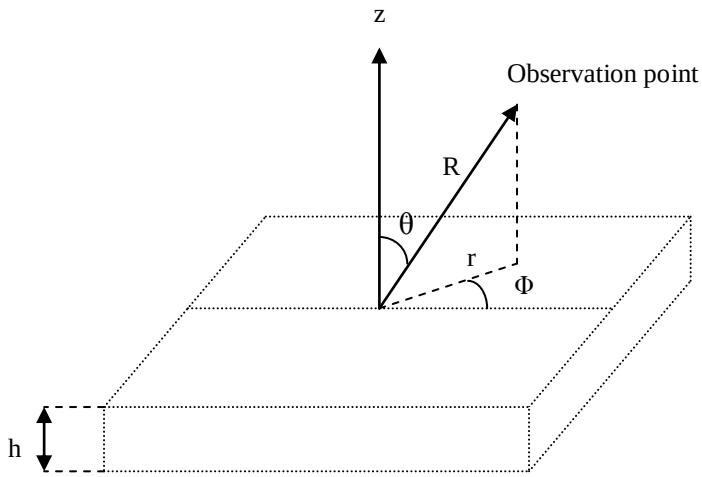

Figure 7. Observation point expressed in cylindrical coordinates, also analyzed by *J, Hannsen Su & R. Vasudevan* [11].

In the case study analyzed in this master thesis, the goal is to induce particle velocity at the observation point. The plate is in contact with air from one side (point force inserted at this side) whereas submerged on water on the other side (observation point). This situation generates different waves inside – outside the plate, with their corresponding speeds:

- Waves inside the plate

1. Compressional wave: $$C_p = \sqrt{\frac{E}{\rho_s(1-\mu^2)}} \quad (1)$$

known as L- Waves.

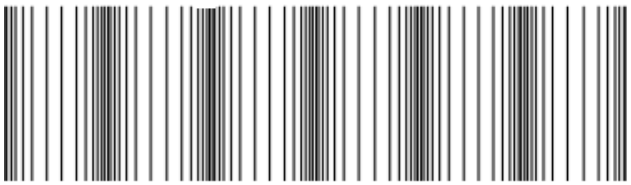

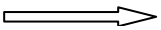

Travelling direction

Figure 8. Wave illustration from *Dr. Jessey* [12]. Also known as push-pull wave

2. Shear wave: $$C_s = \sqrt{\frac{G}{\rho_s}} = \sqrt{\frac{E}{2\rho_s(1+\mu)}} \quad (2)$$

known as T - waves.

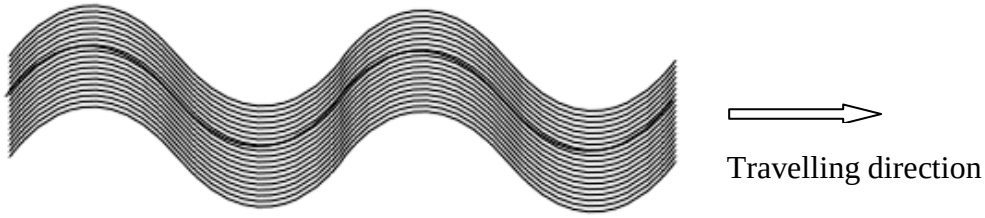

Figure 9. Wave illustration from *Dr. Jessey* [12]. Also called shake wave.

3. Rayleigh wave: $$C_R = \kappa\sqrt{\frac{G}{\rho_s}} \quad (3)$$

where $\kappa = \frac{\pi^2}{12}$ is the shear correction. This wave corresponds to a surface wave travelling inside the solid, and its representation can be seen in figure 10:

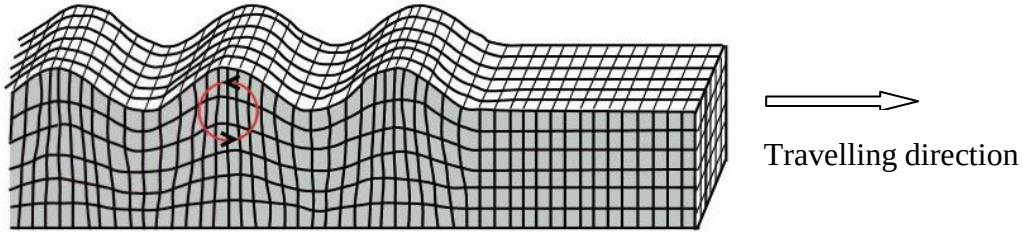

Figure 10. Superficial Rayleigh wave. Reference [12].

Notation from the previous equations:

E [Pa], ρ_s[kg/m^3], μ [dimensionless], G [Pa] are Young's modulus, material density, Poisson's ratio and shear modulus respectively.

- Waves in the surrounding media with water load:

Non dispersive longitudinal waves propagated in the heavy fluid (water), with constant velocity c= 1500 m/s.

The frequency content of the emitted signal is based on the theoretical results of the plate radiation and transducer behaviour, aiming to radiate power more efficiently.

The amplitude of such applied force at first should be limited by 700 Pa, following NATO recommendations, the shape of that signal may content high frequencies inducing bumpy pressure and velocities.

3.2 Thin Plates Theory & bending waves

Firstly, the theoretical analysis reviews the case of a point source applied to one side of a plate (in contact with air both sides). Consider also that the aimed effect is to create a wave for y > 0. This situation is shown in figure 11:

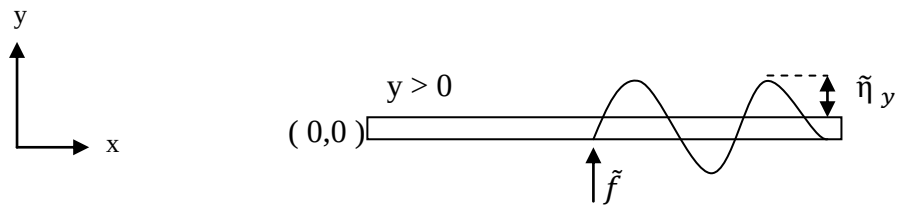

Figure 11.Wave propagated along a plate when applied force F

$$f(x,t) = \tilde{f}e^{-j\omega t} \qquad (4)$$

$$\tilde{\eta} = \eta\, e^{j(\omega t - k_y \cdot y)} \qquad (5)$$

$$\tilde{v} = j\omega\, \tilde{\eta} \qquad (6)$$

$\tilde{f}e^{-j\omega t}$ Applied force [N].

ω,t Angular frequency [rad/s] ω = 2πf, time [s].

$\tilde{\eta}$ $\tilde{v}$ Particle displacement [m], particle velocity [m/s].

k_y Wavenumber in the y axis [m^{-1}].

k is the wavenumber [m^{-1}], defined by the relation between frequency f [Hz] and sound speed c [m/s^2]:

$$k = \frac{\omega}{c} = \frac{2\pi f}{c} \qquad (7)$$

This situation results in waves that are propagated along the x axis of the plate. This effect generates a displacement towards y > 0 as seen in the previous figure 11.

For low frequencies, when the wavelength in the plate is smaller than the wavelength in the surrounding media, the velocity and the pressure in the plate have a phase shift of π/2 radians, leading to propagation in the shape of near fields and no power radiated. At a frequency known as critical frequency, the sound speed is the same for bending waves propagated in the material and waves in the water.

The waves propagated are named bending waves, and their phase speed is as follows:

$$C_B = \sqrt[4]{\frac{\omega^2 B}{m'}} \rightarrow B = \frac{EI}{(1-\mu^2)} = E\frac{h^3}{12(1-\mu^2)} \qquad (8)$$

According to the notes of *Technical Acoustics 1, Wolfgang Kropp* [13].

Where:

C_B bending speed [m/s^2]

B bending stiffness [Nm]

E material Young's Modulus [GPa], μ Poison's ratio [dimensionless].

I moment of inertia [Kgm^2]

m' being the mass unit area $m' = \rho \cdot h$

ρ ,h material density [kg/m^3], material thickness [m]

ω angular frequency [rad/s]

Once calculated the bending speed, the analysis of the bending wavelength is as follows:

$$\lambda_B = C_B / f \qquad (9)$$

The bending wavelengths propagated inside a hull's boat can be estimated from the mechanical properties of the material. The next table 1 shows the main mechanical features of the most common materials used in manufacturing the hull's boat:

	E [GPa]	Poisson's ratio	Density [kg/m^3]	Shear modulus [Pa]
Aluminium	70	0,35	2700	26e9
Fiberglass	45	0,22	2500	18.4e9

Table 1. Mechanical properties of aluminium and fiberglass.

Thus, the wavelengths in aluminium considering a material thickness of 1 cm, data from table 1 and equations (8) - (9) could be approximated as follows:

Frequency [kHz]	**3**	**10**	**50**	**100**
Wavelength λ [cm]	17	9.3	4.1	2.9

Table 2. Bending wavelengths propagated in aluminium.

The theory behind the performance of those waves corresponds to Kirchhoff model, which is only a good approximation for frequencies that accomplish:

$$\lambda_B > 6 \cdot h \qquad (10)$$

Where λ_B, is the bending wavelength [m^{-1}] and the approximation (10) is studied in detail in the *notes of Technical Acoustics* [13].

Considering waves travelling at high frequencies along – through the plate, the equation of motion in the analyzed case is as follows:

$$B\left(\nabla^4 - k_f^4\right) \cdot \tilde{w}(r) = -p(r,0) + \frac{F\delta(r)}{2\pi r} \qquad (11)$$

Where:

B Bending stiffness [Nm]

∇^2 Surface Laplace operator: $\nabla^2 = \frac{\partial^2}{\partial r^2} + \frac{1}{r}\frac{\partial}{\partial r} + \frac{1}{r^2}\frac{\partial^2}{\partial \emptyset^2}$

$\tilde{w}(r)$ Particle displacement.

k_f Flexural wave number [m^{-1}]: $k_f = (\rho_s h\omega^2/B)^{1/4}$

$p(r,0)$ Fluid load on one side: light – heavy fluid considered air – water.

$\frac{F\delta(r)}{2\pi r}$ Harmonic point force.

Equation (11) satisfies the Helmholtz equation for cylindrical waveguides, as explained in *Sound, Structures and their interaction* [9].

If the same observance is pointed towards high frequencies in which the thickness of the plate starts to be comparable with the wavelengths propagated, effects such as rotation inertia and transversal motion occur, and given that those are not consider in the Thin Plates Theory, need for other numerical method arises.

3.3 What kinds of waves are propagated at high frequencies?

When the wavelength is small enough to be on a par with the thickness of the plate, the effects of rotation inertia and transversal motion relative to the mid plane cannot be neglected any longer. In this situation, there are two types of waves generated in the plate: longitudinal and shear waves, called L-Wave and T-wave from now on.

Their propagation towards the surface leads to Rayleigh waves, as studied by *The guideline in the use of different approaches depends on the wavelength – material thickness relationship* [14].

Thus, which theories could be applied to analyze the wave guide at ultrasonic frequency range? Given that the thesis is focused on high frequency range with fluid load on one side, a first approximation analyzing the problem considering the Thick Plates Theory, the following assumptions should be taken into account:

1. Displacements are small compared with the plate thickness;
2. Stress normal to the mid-plane of the plate is negligible and normal to the mid-plane before deformation remains straight but not necessarily normal to the mid-plane after deformation. Statement valid for thick plate theory.
3. Plate with fluid load on one side.

Visually, wave displacements at high frequency inside an elastic plate can be seen in the following figure 12:

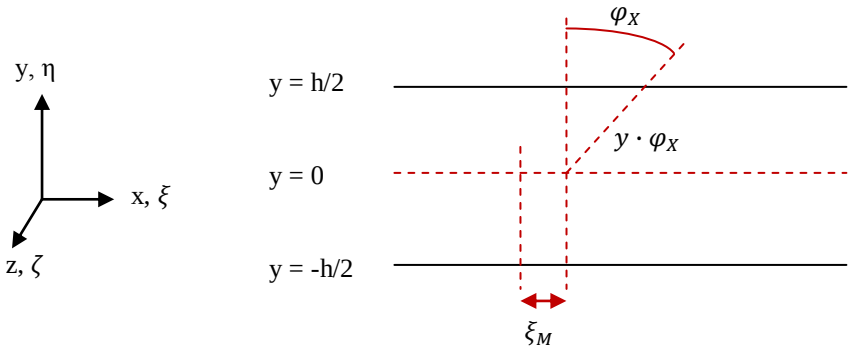

Figure 12. Rotation x-axis through material thickness at high frequency.

Where

x, y, z	Cartesian coordinates
φ_X, φ_Z	Rotation angles at x –z axis respectively.
ξ_M, ζ_M	Displacements along the mid plane y =0.

As examined in *Formulation of Mindlin – Engesser model for stiffened plate vibration* [15], a study in 2D considering the rotation angles generated at the Cartesian axis x and y, result in following displacements:

$$\xi = \xi_M + \varphi_x \, y \qquad (12a)$$

$$\zeta = \zeta_M + \varphi_Z \, y \qquad (12b)$$

The displacements shown in equation (12a) and (12b) and previously illustrated in figure 12, are not taken into account in the Thin Plates Theory, thus need for other numerical models arises.

3.4 Thick Plate Theory - Mindlin models

For the situation of ultrasound propagation with water load, the Mindlin model has been chosen to observe the physics behind. This model is also known as MPT. Before proceeding to its mathematical development, in the next part 3.4.1 the use of this approach is justified based on the frequency range under study briefly compared with other theories.

3.4.1 Analysis of the frequency validity for different approaches

In this part an observance throughout the aimed frequency range takes place.

(1) Lower frequency limitation, obtained by comparing MPT with the Thin Plates Theory.

Although there is no low frequency limitation for the MPT, the lower frequency applied at this study coincides with the higher frequency limitation for Thin Plates Theory for which negligible error is introduced. This frequency shows the moment at which rotation inertia and transverse motion starts to be noticeable. Given that those facts are not considered in the Thin Plate Theory this approach lacks accuracy from those frequencies. The limit frequency is represented by the bending wavelength:

$$\lambda_B > 6h \qquad (13)$$

Being λ_B the wavelength of the bending waves.

According to the notes of *Technical Acoustics 1, Wolfgang Kropp* [13].

(2) Higher frequency limitation, obtained by comparing the MPT with the Leaky Lamb Waves a.k.a LLW-Theory.

So as to determine how accurate MPT is relative to ultrahigh frequencies, a preliminary analysis of the modal behaviour takes place considering the ratio between material thickness – wavelength.

On one side the use of different approaches depends on the wavelength – material thickness relationship, thus according to *N.G. Stephen* [16], the MPT determines that there are three frequency ranges based on how similar the natural stationary wave's resonance –phase velocity is to the lower flexural vibration mode. Based on this study, three frequency ranges can be seen relative to the existence of:

- Shear modes, called SH.
- Thickness shear modes, referred as ω_2
- Thickness twist modes, referred as H.

Note: the mode's notation has been taken from *Stephen* [16].

When frequency is increased those modes start progressively being noticed, which means that at the frequencies coinciding with Thin Plates Theory upper frequency limit SH modes appear. Higher frequencies produce the existence of thickness shear modes and finally for ultra-high frequency, thickness twist motion appears leading to the excitation of these modes.

For the analysis of the MPT's higher frequency limit, this approach is compared to the Leaky Lamb Waves theory, LLW. In brief, the LLW approach states that there are mainly L- waves and T – waves generated, from which T- waves do not propagate in water given the low shear strength (viscosity), which can be reviewed in *Determination of the shear strength and modulus of water at low flow velocities* [17]. The combination of the propagation of those waves results in a wave pattern in which A/S, anti-symmetric / symmetric, modes can be monitored. A deeper explanation of this theory can be found at the Appendix D.

In order to determine how accurate MPT is at ultra high frequencies, this theory is compared to the waveguide described by LLW approach. This comparison can be clearly seen in the next figure 13:

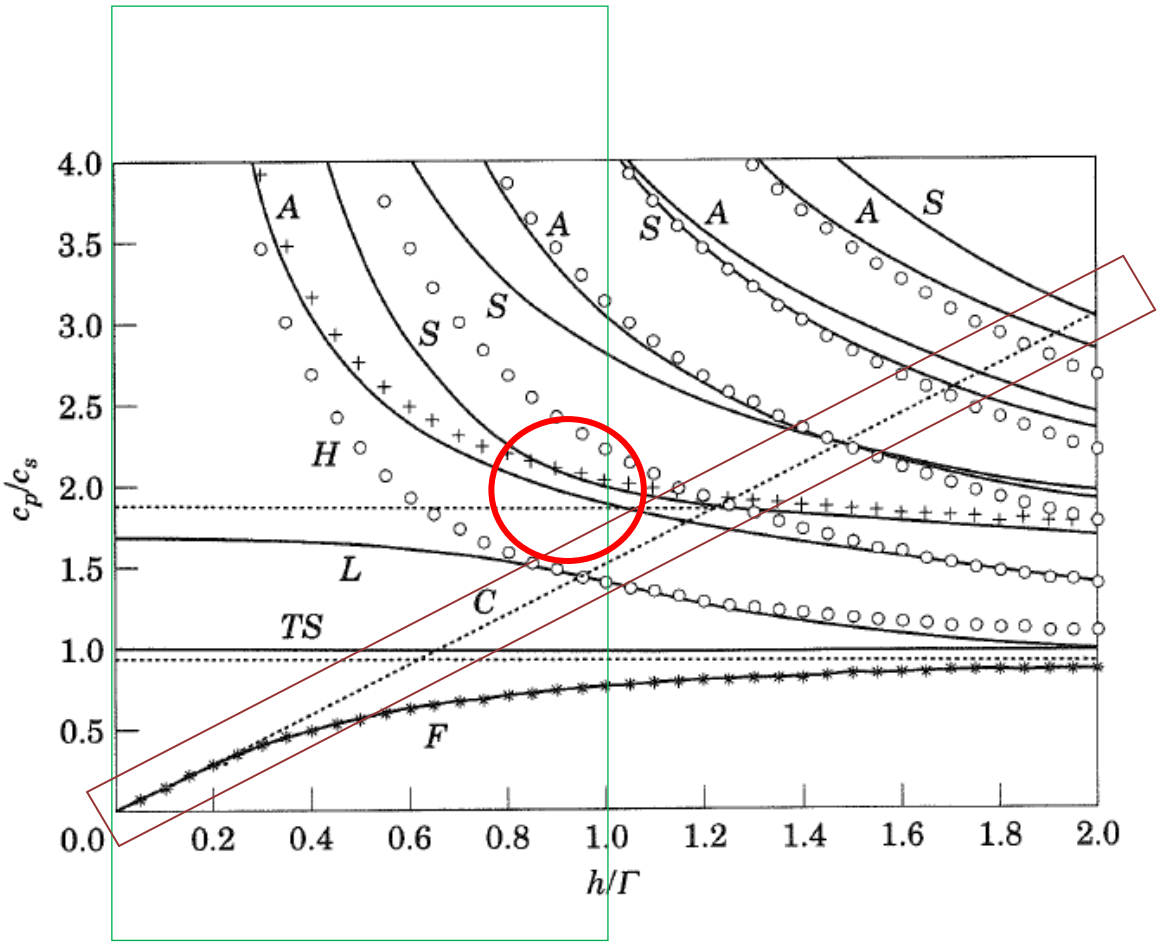

Figure 13 Dispersion diagram for the waves observed by the Thin Plates Theory, MPT, Leaky Lamb Waves approach. Horizontal axis: plate thickness – half wavelength, vertical axis: a-dimensional phase velocity. Figure taken from *Stephen* [16].

Notation:

* ω_1 mode ° SH mode + ω_2 mode corresponding to MPT.

--- Rayleigh superficial wave

Γ half wavelength: $\Gamma = \lambda/2$

h material thickness.

C waves described in Thin Plates Theory. Framed in red.

F, TS, L, H Flexural wave, thickness shear wave T-wave, L-Wave, H mode observed in MPT.

A, S Asymmetric , Symmetric modes analyzed in LLW Theory. Thick line.

Dividing the conclusions according to the thickness – half wavelength ratio:

There is no clear tendency for the modal behaviour in the study of the ω_2 (thickness shear mode). The diagram shows that according to MPT this mode, for $h/\Gamma << 0.5$, coincide to an anti-symmetric mode but as frequency increase MPT starts to perform as a symmetric (circle brought out on figure 13). This fact could be explained, according to *N. G. Stephen* [16], because of the excitation of various modes simultaneously inside the elastodynamic material. MPT does not consider that fact so that induces noticeable error at that situation. It could be said that the higher

frequency limit for the application of the MPT coincides with the 0-order anti-symmetric / symmetric modes called A0 / S0.

In this situation for an aluminium plate with characteristics shown in table 1 and thickness 1 cm:

Thin Plates Theory maximum frequency for 10 % accuracy error:	24 kHz.
Thick Plates Theory lower frequency (equation 9):	15 kHz.
LLW 0-order modes A0 – S0 (analyzed in Appendix D):	>> 150 kHz.

For the frequency range under observance [20 kHz to 90 kHz], the numerical model selected is Thick Plates Theory as well known as Mindlin Plate Theory of MPT.

3.4.2 Mindlin Plate Theory approach.

The waveguide is based on the propagation of L- waves and T – waves. Applying water load, T- waves do not propagate in water given the low shear strength (viscosity), which can be reviewed in *Determination of the shear strength and modulus of water at low flow velocities* [17]. This fact is taken into account when analyzing plate radiation with water load. Nevertheless, the radiation effect is minimum at frequencies below the coincidence frequency: frequency at which phase speed inside the plate is equal to sound speed in the surrounding media (existence of supersonic wave).

$$k = k_f \qquad (14)$$

k wavenumber in the surrounding media $k = 2\pi/\lambda$ [m^{-1}]

k_f flexural wavenumber $k = 2\pi/\lambda_f$ [m^{-1}]

For non- water load, the supersonic wave coincides with the flexural wave travelling inside the material. Introducing water load, this fact is fulfilled in the presence of compressional wave in the water, as a consequence:

$$\omega_c = \frac{\sqrt{12}\,C^2}{hC_p} \qquad (15)$$

Being c, c_p: sound speed in the water, compressional speed in the plate.

As the analysis is carried out in cylindrical co-ordinates, Hankel transform (Appendix A) is applied as 2-D transform, by using the transform parameter γ following *Ultrasonics: fundamentals and applications* [18], the equation of motion leads to:

$$\left[B\nabla^2 - \frac{\rho_S h^3}{12}\frac{\partial^2}{\partial t^2}\right]\left[\nabla^2 - \frac{\rho_S}{k^2 G}\frac{\partial^2}{\partial t^2}\right] w = -\tilde{p}(r,0) + \frac{F}{2\pi}$$

$$B\left(\gamma^4 - k_f^4\right)\tilde{w}(r) = -\tilde{p}(r,0) + \frac{F}{2\pi} \qquad (16)$$

$\tilde{p}(r,0)$ Fluid load on one side: light – heavy fluid considered air – water.

ρ_S material's density [kg/m^3]

k wavenumber [m^{-1}]

G shear stiffness [GPa]

h material's thickness [m]

B bending stiffness [Nm]

$\tilde{w}(r)$ Particle displacement (RMS)

k_f Flexural wave number [m^{-1}]: $k_f = (\rho_s h\omega^2/B)^{1/4}$

In the study case axisymmetric pressure fields are analysed with cylindrical coordinates as shown in figure 7. Thus, given transformed variables z, R and applying continuity at the boundary the previous equation (16) yields to:

$$\rho\ddot{\tilde{w}}(r) = -\frac{\partial\tilde{p}(r,z)}{\partial z}\ at\ z = 0 \qquad (17)$$

Therefore, two equations for two unknowns: pressure and displacement. Solving the previous equations, according to *J. Hannsen Su and R, Vasudevan* [11], one can arrive to the relationships of pressure – displacement:

$$\tilde{p}(\gamma,z) = -i\omega Z_a(\gamma)\tilde{w}(\gamma)e^{iz\sqrt{k^2-\gamma^2}} \qquad (18)$$

$$\tilde{w}(\gamma) = \frac{iF}{4\pi\omega(Z_a+Z_p)} \qquad (19)$$

$$Z_a = \widetilde{Z_a}(\gamma) = \frac{\rho\omega}{\sqrt{k^2-\gamma^2}} \qquad (20)$$ Impedance in the surrounding media.

$$Z_p = \widetilde{Z_p}(\gamma) = -i\omega m\frac{[1-(\gamma^2-k_p^2)(\gamma^2-k_R^2)/k_f^4]}{1+\left(\frac{h^3}{12}\right)(\gamma^2-k_c^2)(k_R^2/k_c^2)} \qquad (21)$$

Equation (21) refers to the plate impedance at the boundary.

k_R Rayleigh wavenumber [m^{-1}]

k_C Medium wavenumber [m^{-1}]

k_P Compressional wavenumber [m^{-1}]

ρ Density of water [kg/m^3]

Where the wavenumbers k are calculated following equation (7) based on the different waves generated, already explained in part 3.1.

Similarly, following the mathematical approach explained by *J. Hannsen Su and R, Vasudevan* [11], displacement can be obtained as:

1. $\frac{\omega}{\omega_c} \ll 1 \qquad k_f r \gg 1 \qquad w(r) \approx \left(\frac{F}{10}\right)\sqrt{\frac{2}{\pi B r \rho}}\, e^{(i\gamma r - i\pi/4)}$ (22)

This is an ultra low frequency approximation where the assumptions applied are no inertia & fluid compressibility and the wave amplitude in the far field is proportional to the bending moment and fluid density (already stated that no bending waves are propagated under the range of interest).

2. $\frac{\omega}{\omega_c} < 1 \qquad w(r) \approx \frac{\frac{iF}{\omega Zp} H_0(\gamma r)}{\left(\frac{\gamma}{k_f}\right)^2 \left\{ 1 + \frac{\varepsilon}{\left[4\Omega\left(\frac{\gamma}{k_f}\right)^2 \left[\left(\frac{\gamma}{k_f}\right)^2 - \Omega\right]^{3/2}\right]} \right\}}$ (23)

H_0 hankel function first order, explained in detail Appendix A.

For $\gamma = k_f \sqrt[4]{1 - \frac{\varepsilon}{\sqrt{\Omega(1-\Omega)}}}$ and $\Omega = {}^{\omega}/_{\omega_c}$

Approximation for low - medium frequencies.

3. $\frac{\omega}{\omega_c} > 1$

The previous approximations where made by solving inverse Hankel transform over the contour C (explanation appendix A), by the method of stationary phase as explained in *Sound, structures, and their interaction* [9].

In case 3. Aimed situation for high frequency range: displacement must be calculated through the numerical integration over real values of γ:

$$\widetilde{w}(r) = \frac{iF}{4\pi\omega} \int \frac{H_0(\gamma r)\gamma\, d\gamma}{(Z_a + Z_p)} \qquad (24)$$

When solving the 10th order γ polynomial detailed in Appendix A, only the values of γ with positive real and imaginary are considered, leading to three waves:

(1) Subsonic wave travelling along the plate surface, inside the plate.

(2) Decreasing wave with increasing frequency, in the water.

(3) Supersonic wave decreasing faster for frequencies above the critical frequency, in the water.

Given that displacements and velocities are observed in the far field (few centimeters from the plate surface), the subsonic wave has no influence and only the supersonic wave is taken into account. Thus, the particle velocity can be studied as:

$$\tilde{\dot{w}}(\gamma) = -i\omega\tilde{w}(\gamma) \qquad (25)$$

According to *J. Hannsen Su and R, Vasudevan* [11], analysing the influence of supersonic wave in the far field, and solving the previous equations by numerical calculations, the pressure in the far field can be obtained as:

$$p(R,\theta) = -ikF\frac{e^{ikR}}{2\pi R}cos\theta\left\{1 - ikh\left(\frac{\rho_s}{\rho}\right)\cos\theta\frac{1-(\omega/\omega_c)^2[\sin\theta^2-(c/c_p)^2][\sin\theta^2-(c/c_R)^2]}{1+(k^2h^2/12)(c_p/c_R)^2[\sin\theta^2-(c/c_p)^2]}\right\}^{-1} \qquad (26)$$

c_R Speed of the Rayleigh wave [m/s].

c_P Speed of the compressional wave [m/s].

θ Angle, cylindrical coordinates according to figure 7.

After all, the plate response in the far field relies on a shear corrected wave under the influence of the water load, having pressure amplitude:

$$A \propto {}^{1}/_{\sqrt{r}} \qquad (27)$$

A, r amplitude and distance

Once obtained the sound pressure in the far field, the emitted power and thus the radiation can be examined. Acoustic power evaluation:

$$P = \frac{\pi R^2}{\rho c}\int_0^{\pi/2}|p(R,\theta)|^2\sin\theta\, d\theta \qquad (28)$$

$$\sigma = {}^{P}\Big/_{\pi\rho c\int_0^{\infty}|\tilde{v}(\gamma)|^2\gamma d\gamma} \qquad (29)$$

The radiation efficiency is calculated directly with the velocity in the transform domain, by applying Parseval's identity, as analyzed by *Digital Signal Processing* [19].

$$\int_0^{\infty}|v(r)|^2 r dr = \int_0^{\infty}|v(\gamma)|^2\gamma d\gamma \qquad (30)$$

So as to study the coherence between measurements and theoretical approach, radiation with and without water load has been analyzed, although in the following pictures results with one side water load are shown.

Real part - Phase displacement over distance for supersonic wave by means of the low frequency approximation.

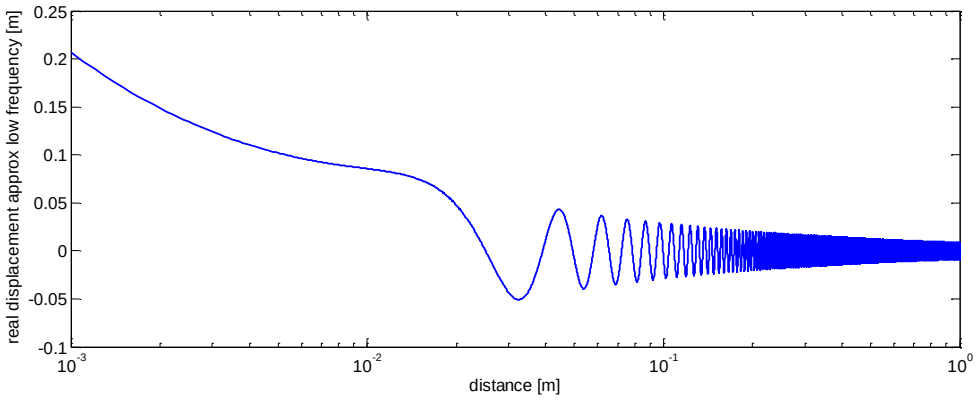

Figure 14. Displacement low frequency approximation, input force amplitude 1 N.

- Waves performance for the high frequency approximation.

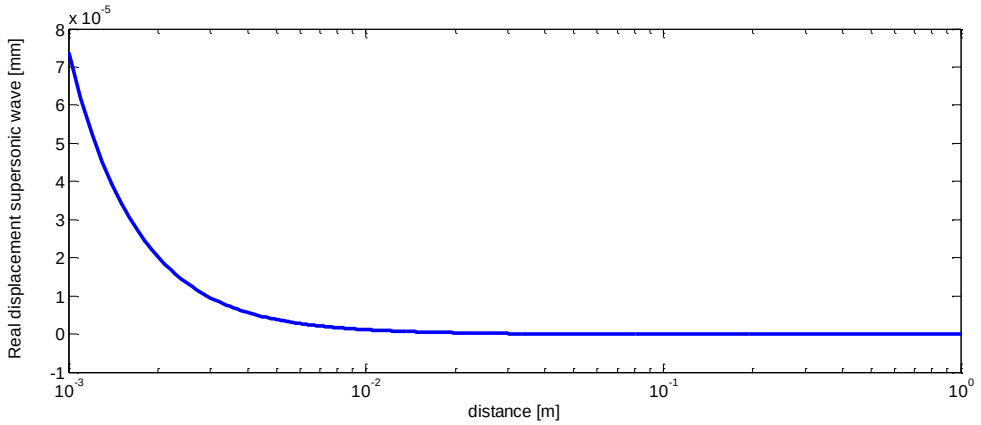

Figure 15. Real displacement supersonic wave at 80 kHz, input force amplitude 1 N .

Figures 14,15 aid visually to analyze the wave displacement pattern and amplitude. Nonetheless, the next figures are clearer so as to check the sound properties over distance.

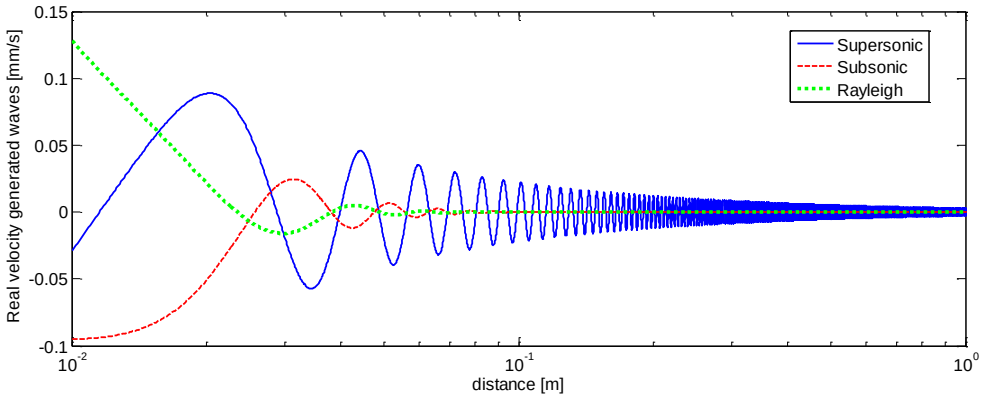

Figure 16. Real velocity high frequency, input force amplitude 1 N.

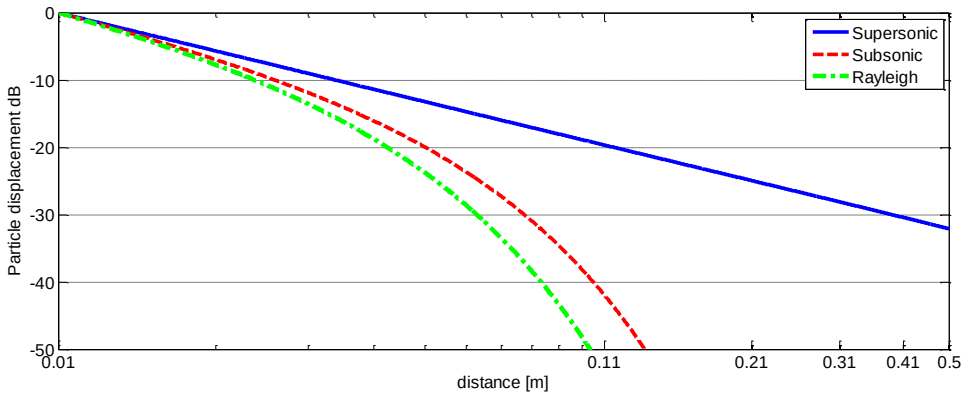

Figure 17. Particle displacement relative to amplitude at 1 cm distance,

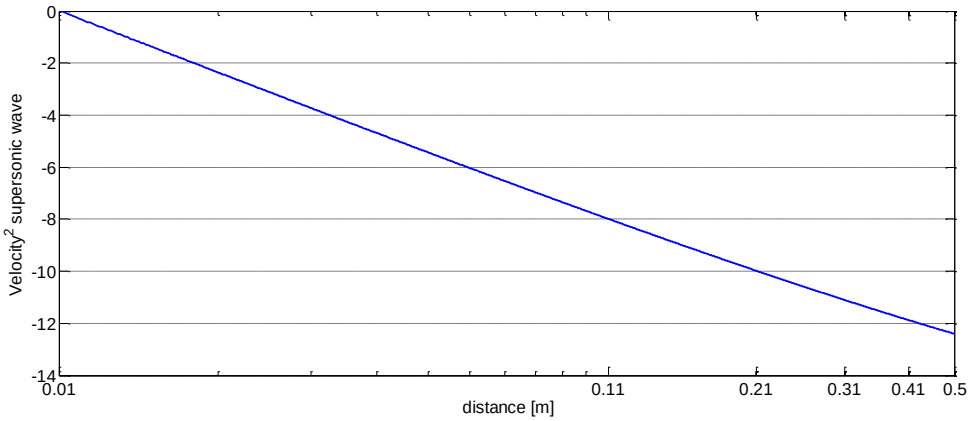

Figure 18 Squared velocity - high frequency model- relative to amplitude at 1 cm distance

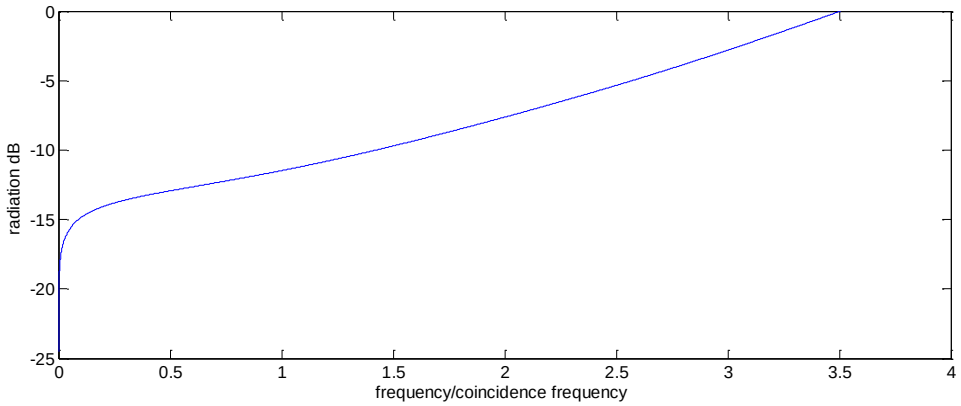

Figure 19 Radiation dB with water load regarding multiples of the coincidence frequency.

As it can be seen in difference with the Thin Plates Theory, the radiation efficiency tendency is in increasing for higher frequencies. The shape obtained in the case of water loading on one side differs to the common Thin Plates Theory in the sense that the maximum radiation is not achieved at the coincidence frequency but its tendency is increasing with higher frequencies. The curve for frequencies below the coincidence frequency is explained by the fact of the water performing as an added mass; whereas for frequencies above coincidence frequency, the radiation increases relying on the propagated supersonic wave. Theoretically, the radiation should accomplish unity, although given that the supersonic wave is decreasing with distance, its contribution is not so outstanding at very high frequencies.

In order to extrapolate the results on a ship hull, numerical studies can be carried out in line with *Ship Hull Vibration* [20], in which the main calculations are based on added virtual weight due to the water load and machinery and adjustment of this value to given theoretical studies. Finally that value is combined with given vibration profiles considering as well shear forces and acceleration at the nodes.

Regarding *N.G Stephen* [16], Mindlin models are accurate in prediction for the first order thickness shear mode determined while for multiples of such frequency LLW

(Leaky Lamb Waves), fits more precisely phase velocity estimation.

3.5 Environmental impact assessment

The ultrasounds approach proposed in this thesis has been observed to ensure environmental friendly actions, both from the frequency range and the signal amplitude points of view. Thus, the working frequency range has been selected to accomplish low acoustic underwater pollution – high attenuation in distance- and avoid bubbles implosion, also the amplitude of the applied signal has been limited by the NURC Rules and Procedures directives. On the other side, as the tests were carried out with several cultures of living organisms – cyprids, those were released in the sea when the measurements were over to preserve their lives.

3.5.1 Sonic cracking

One of the most effective procedures to prevent living organisms to get attach to the hull could be producing bubbles that travel along the hull surface. For that purpose, ultra high frequencies in the range of MHz must be in use, which can lead to phenomena such as sonic cracking. This could result in bubbles implosion leading to killing of microorganisms and materials erosion, this process also known as sonification, is widely used in ultrasound applications for cleaning purposes such as algae eradication, but is has been dismissed in this study case.

In the next figure 20, frequency ranges according to bubbles diameter are shown. It can be observed that by applying ultrasounds up to 100 kHz –cost- effective for a ultrasounds device on a boat-, the bubbles that could be cracked would have a diameter bigger than 10 cm. Considering that the balanus larvae are 0.1 cm diameter, a frequency higher than 10^9 Hz would be necessary to disturb them violently (or even kill them). This analysis has been carried out assuming that the bubble membrane performs as lipid encapsulation and applying the resonance bubble frequency as stated in Sonic cracking of blue – green algae, as analyzed in *Applied acoustics volume 70* [21]

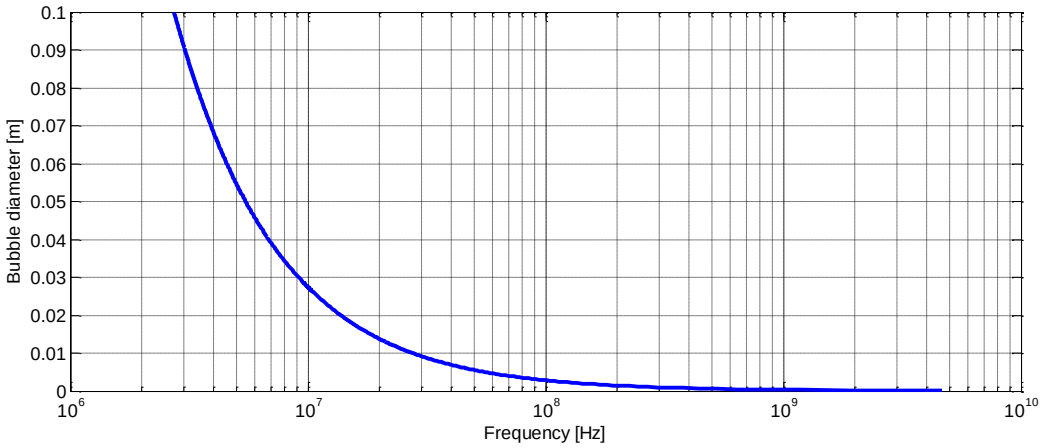

Figure 20. Microbubbles cracking for applied pressure 700 pa.

The axes show the diameter bubble that can be burst at different applied frequencies.

To sum up, the applied signal in this thesis contains frequencies << 10^9 Hz, no bubbles implosion occurs.

3.5.2 Sound absorption in the sea (in case the device is placed in the water facing the hull).

Being aware of the current acoustic pollution on the sea, the emitted signals has been analyzed so as to accomplish great attenuation over distance, given that the goal is to produce disturbances only at a surface few centimetres around the hull.

Seawater is compound by boric acid, magnesium sulphate and fresh water. Those chemicals affect the sound absorption depending on the concentration. Regarding studies following *Marin Akustik* guidelines [22], those influences are as follows:

- Boric acid $B(OH)_3$ contribution

$$A1 = \frac{8.86}{c}\ 10^{0.78pH-S}\ \left[\frac{dB}{Km \cdot kHz}\right] \qquad (31)$$

$$P1 = 1; \quad f_1 = 2.8\ (\frac{S}{35})^{0.5}\ 10^{4-1245/\theta} \quad [kHz] \qquad (32)$$

A1 Auxiliar parameter based on absorption per distance- frequency.

P1 Auxiliar parameter based on absorption per depth.

c sound speed in water [m/s]

f , f_1 Observed frequency and the relaxation frequency for boric acid respectively.

S [ppm] is salinity; D[m] depth; and pH (acidic water index) .

- Magnesium sulfate $MgSO_4$ contribution

$$A2 = \frac{21.44S}{c}\ (1 + 0.025T)\ \left[\frac{dB}{Km \cdot kHz}\right] \qquad (33)$$

$$P2 = 1 - 1.37\ D10^{-4} + \ 6.2\ D^2 10^{-9}\ ; \qquad f_2 = \frac{8.17\ 10^{(8-1990/\theta)}}{1+0.0018(S-35)}\ [kHz] \qquad (34)$$

A2: Auxiliar parameter based on absorption per distance- frequency.

P2: Auxiliar parameter based on absorption per depth

f -f_2 Observed frequency and the relaxation frequency for $MgSO_4$ respectively.

.

- Fresh water absorption for T ≥ 20ºC

$$A3 = 4.937 \cdot 10^{-4} - 2.59 \cdot 10^{-5}T + 9.11 \cdot 10^{-7}T^2 - 1.50 \cdot 10^{-8}T^3 \left[\frac{dB}{Km\ kHz}\right] \quad (25)$$

A3 Auxiliar parameter considering absorption depending on temperature.

The previous analysis was developed by Francoise and Garrison (1982) as explained in *Marine Akustik* [22]. The final calculation sums up the above contributions in order to calculate the absorption α, for each frequency given specific environmental conditions:

$$\alpha = \frac{A1P1f_1f^2}{f^2 + {f_1}^2} + \frac{A2P2f_2}{f^2 + {f_2}^2} + A3P3f^2 \quad (35)$$

Environmental values account in the calculations (according to average values on the West Coast for Sweden):

Water speed	Average temperature	Salinity	pH
1500 m/s	18 ºC	30 ‰	7.8

Table 3. Water parameters taken into account for the calculations shown in figure 21.

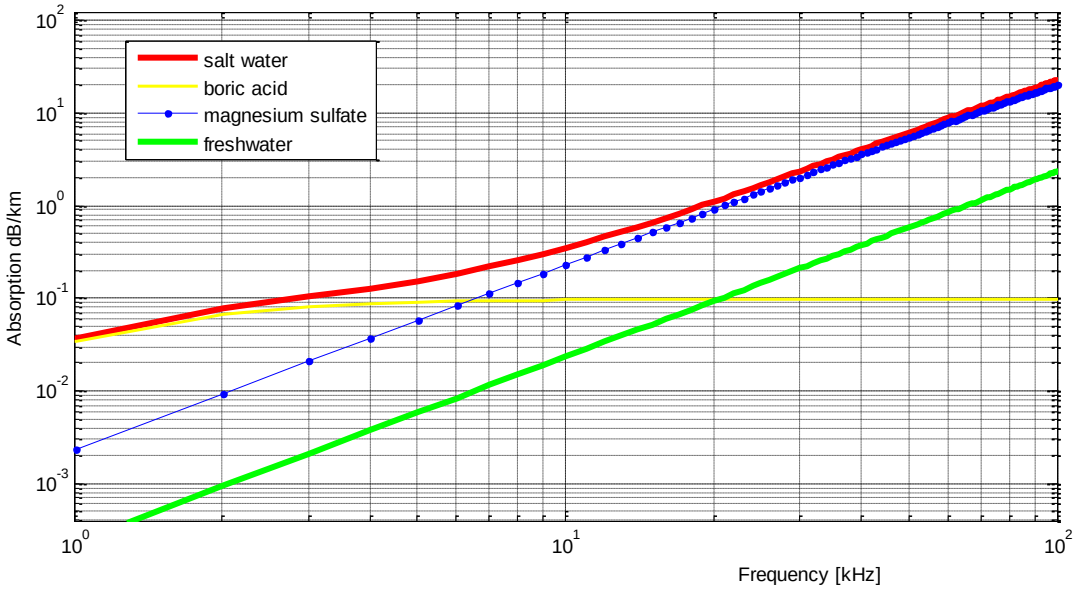

Figure 21. This figure shows the increase in sound absorption with higher frequencies, data to take into account to avoid increasing noise propagation at long distance from the device.

In the previous figure 21, it can be seen the relative absorption produced at different frequencies. In the frequency range under study of this thesis, frequencies above 20 kHz, the diagram shows salt water absorption is more than 1dB/kilometer (horizontally). Thus, the following figure gives an idea of the necessity of using signals in the high frequency order so as to reduce the acoustical pollution in the sea:

Even when using a signal of 70 kHz the attenuation introduced is around of 10 dB per km re 1 µPa.

4 Experiments

4.1 Biological experiments & equipment

The main goal of this master thesis has been to observe the actual behaviour of the living organisms towards the applied signal, for that reason the biological measurements were done in cooperation with researches from Sven Lovén Centrum för Marina Vetenskaper: Matz Berggren [3]from Lovéncentret Kristineberg - biological assessment - and Martin Ogemark – cyprids culture – from Lovéncentret Tjärnö as well as asssistance from Ingemar Martinsson, Volvo Penta AB.

In order to study the effect of induced vibrations on a plate so as to prevent the attachment of barnacles balanus improvisus, these organisms can be obtained at the cyprid stage (when the animal has accomplished the larvae process and looks for a surface to settle down). The advantages of this stage are that balanus feed from the lipids stored in their bodies and no specific requirements of nutrients are needed. The selected specie is the one most common on west coast of Sweden and can reproduce at the conditions of low – medium water temperature (around 16 – 18 ºC) and salinity around 15 – 20 ‰.

According to Matz Berggren, it takes around 8 – 10 days for the cyprids to become juvenile barnacles, thus to have results for the experiment. The whole experiment should be repeated at least 3 times in order to have enough data to drop conclusions as well as to make sure that the delivery of cyprids was ok. The amount of cyprids needed depends on water volume of the testing tanks, the first set up of the experiments has been based on 4 tanks:

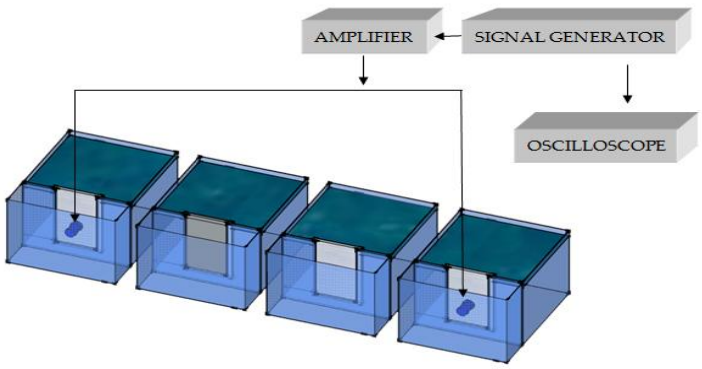

Figure 22. General overview of the bioacoustics measurements set up. To be explained in detail in this section.

From figure 22, the tanks are classified from left to right (tank 1, 2, 3, 4).

- Tank 1: inside aluminium & Plexiglas plates are placed. The aluminium plate simulates the hull and the Plexiglas plate is a dummy plate to check the culture process, also as the vibrations were applied in one of the plates, it could be checked how the vibrations affect directly the plate surface and the sound propagation towards the other plate.
- Tanks 2 & 3: containers without any acoustical device. Located Plexiglas and aluminium plates correspondingly. The selection of Plexiglas took place given that this material seems to be very attractive for barnacles to attach because of its mechanical properties. Therefore, Plexiglas has been used as a reference of the culture success.
- Tank 4: this aquarium contains an aluminium plate with applied ultrasound signal identical to the other aquarium. The aquariums were built on glass so as to ensure that no polluting substances leak in the water, disturbing the organisms.

The water in the aquariums has been under control so that salinity and temperature have been constant, matters regarding salinity gradient from shallow waters, in case that the water comes from Volvo Penta AB facilities at Krossholmen, have been considered: water extraction from depths minimum 30 m.

Although at first tanks water renewal was advised every 3 days, finally this process has not taken place given that the organisms waste is negligible and the renewal process could be very disturbing for the cyprids.

Finally, plankton nets were placed covering the inner surfaces of the tank in order to prevent balanus from attaching on them thus pushing them to attach to the test plates. The hole's diameter of such nets is 200 μm: given that cyprids search for a surface walking on the first antenna, which size in smaller than the net holes, making the net not a comfortable place to establish themselves.

- **Facilities set up**

The room in which the measurements take place must have a constant temperature of 15 ºC (both atmosphere and water inside the aquariums) and the light conditions must simulate real environment: light – dark cycles of 8 hours. For that purpose a timer is set up to provide daylight from 8 a.m. to 20 p.m.

- **Aquariums requirements**

The size of the aquarium has been studied so as to minimize reverberation compromising with the cyprid's culture budget. The goal is sound energy to be dissipated before arriving to the walls in order to get a general sound behaviour as close as possible to the real situation of a boat placed on the harbour. Preliminary estimation according to sound propagation in different media is given:

Frequency (kHz)	10	20	50	80	100
Wavelength water (cm)	15.0	7.5	3.0	1.8	1.5
Wavelength air (cm)	3.43	0.17	0.69	0.43	0.34

Table 4. Calculated wavelengths of waves in different media, depending on their frequency.

Note: Finally the noise inside the aquarium produces noticeable reverberation as it will be seen in the Results part.

Besides, the design of the aquariums provides an empty space where the transducer is located to avoid water load on both sides of the test plates which can change the radiation pattern on the plates. Final design is as follows:

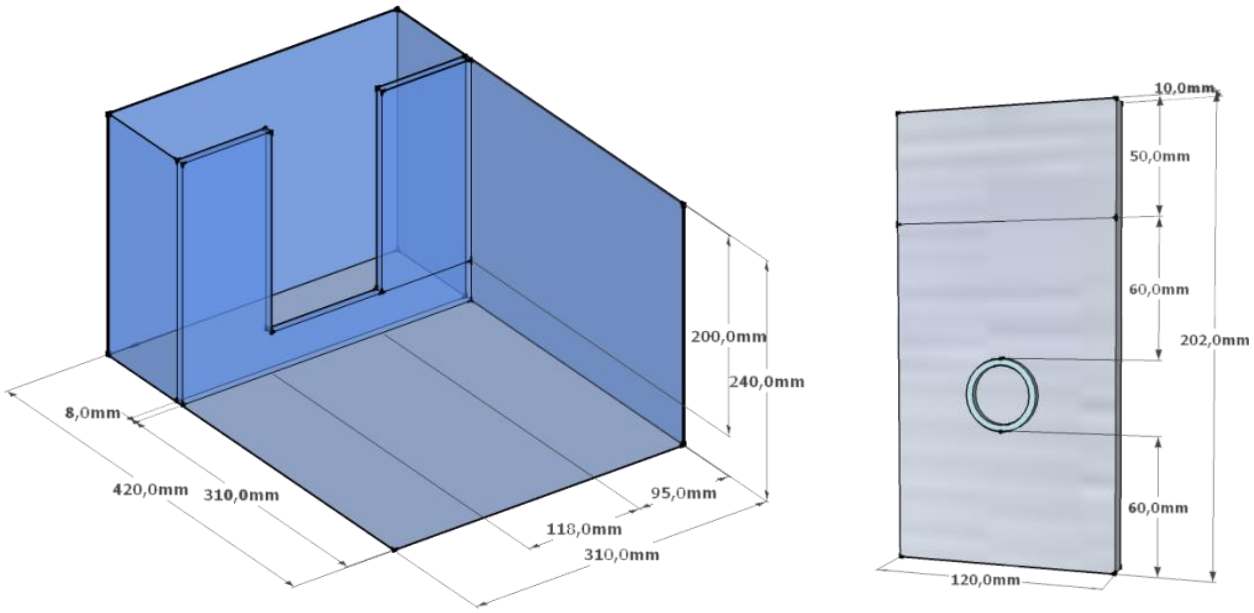

FIgure 23. Aquarium dimensions, total volume 18 liter.

Figure 24. Plate size and placement of the transducer ring regarding tank inner glass structure in order to center the sound emission in respect of the aquarium.

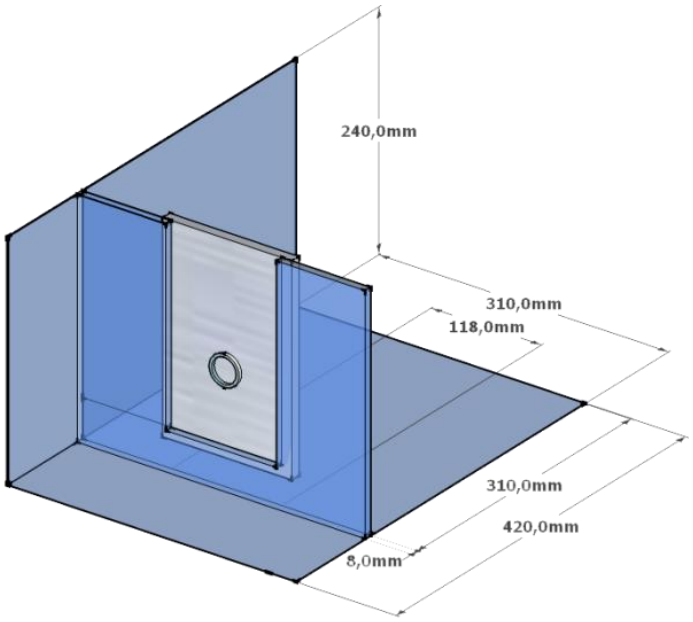

Figure 25. Plate location inside the aquarium.

The silicon that has been used to glue the plates – nets – inner structure is *Silicon Glas Bostik* [23]. This specific type was selected given that common acid components are substituted by vinegar-kind chemicals which make the silicon less polluting and more suitable for aquariums. Nevertheless, before refilling the aquariums the silicon was dried and then washed off with running water for 8 hours to ensure pollutant –free environment.

- **Requirements aluminum testing plates**

The aluminium testing plates used for the aquarium measurements were taken from the same material bar which manufacturer's specifications can be review in Appendix B. Plate's surfaces were cleaned but remained unpainted so as to avoid the influence of antifouling coating. In order to reduce both oxidization processes on the surface and water pollution, the selected material contains high aluminium purity and low amount of copper, oxidization process was checked submerging one of the plates in a water tank for a week.

Note: that several ultrasounds antifouling manufacturers recommend applying the device on a hull with a layer of antifouling coating.

- **Acoustical emitting chain**

In order to drive the ultrasound transducer, first of all electrical characterization was carried out to find out the device's resonance and frequency response of the acoustical chain. Previous to this study,a review of Ultra – 10 features takes place given by the original manufacturer *Flexidal Technics* [24].

- Ultra – 10 AC Transducer: Power consumption 700 mA_{MAX}, when driven by 12 V_{AC}
- Ultra – 10 AC Module: 100 - 240v AC (50 – 60 Hz), power consumption 15 watts.

Next, electrical characterization took place, by performing a sinusoidal sweep from 9 kHz to cut off frequency of 100 kHz. The goal was to analyze the electrical features of the system based on the feeding chain (signal generator & amplifier) and the ultrasounds transducer. The current was measured in series with the transducer, while the voltage in parallel to the generator. Note that the input voltage remained constant to 108 $V_{RMS\ DC}$. The following frequency response was observed:

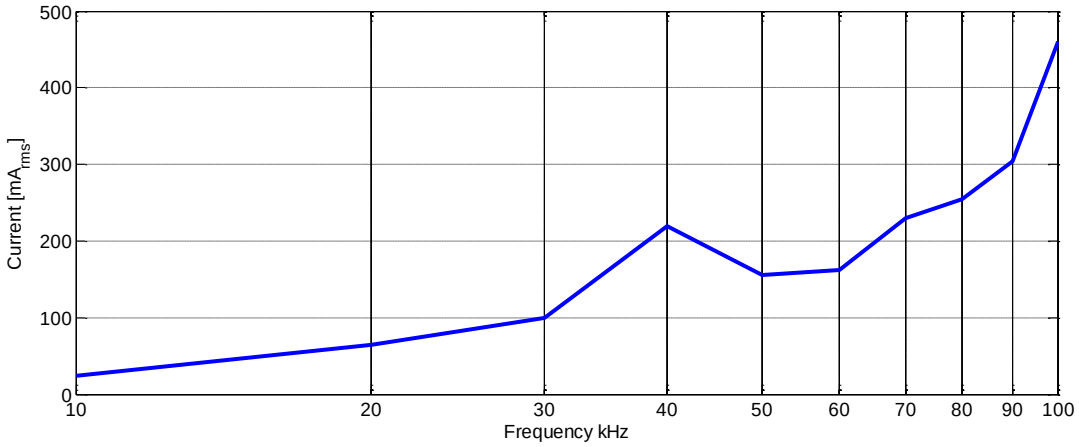

Figure 26. Current measured at the ultrasounds transducer at different frequencies.

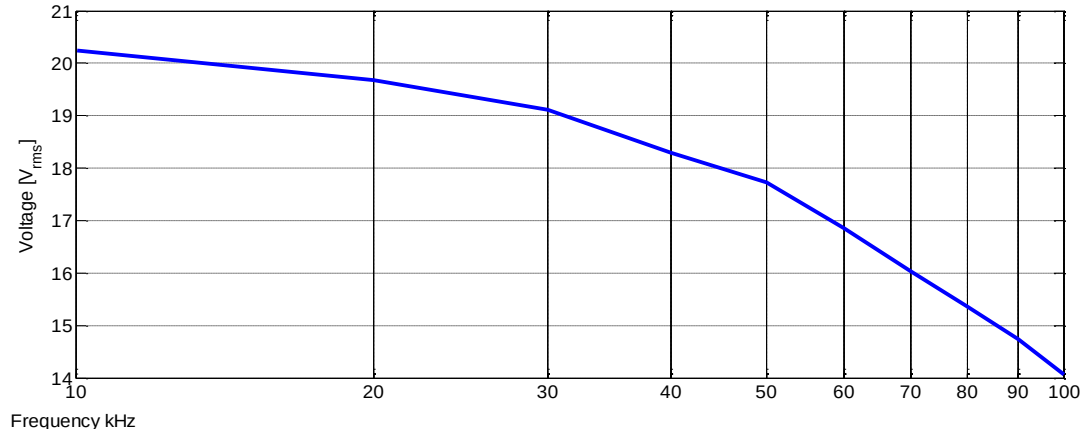

Figure 27. Voltage drop observed at the transducer.

The values expressed in these figures 26 -27 are shown in table 5.

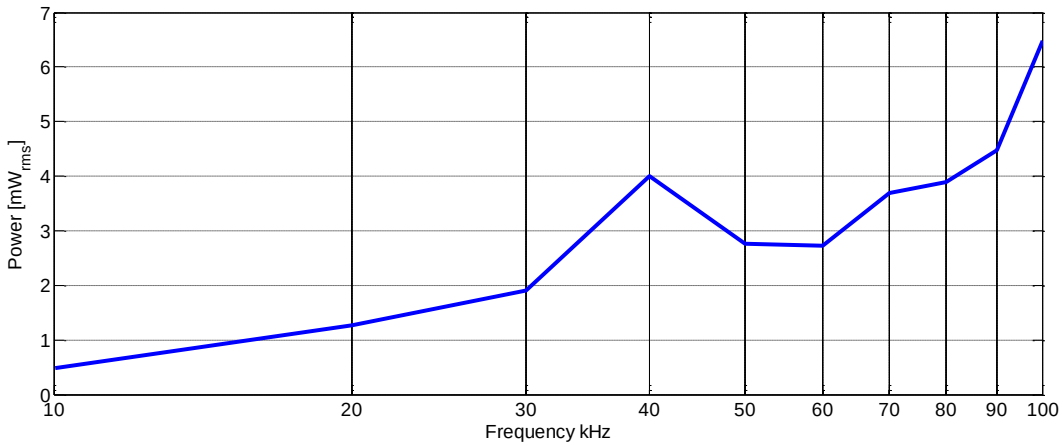

Figure 28. Power obtained at the transducer as a result of the current and voltage drop measured.

Given the lack of FFT Analyzer at this stage, the measurement took place by playing one by one all the frequencies to understand the performance in that frequency range, thus signal resolution [10, 20... 100 kHz]. The acoustic chain is the one specified in table 5.

Observing the results, there is a transducer resonance at 40 kHz which should be within the excitation range. Therefore, in order to attack resonance frequency sub – harmonic and super – harmonics at multiple frequencies, the selected working range has been chosen to be from 20 to 90 kHz, given that from 90 kHz onwards, the voltage drops dramatically.

- **Physical set up**

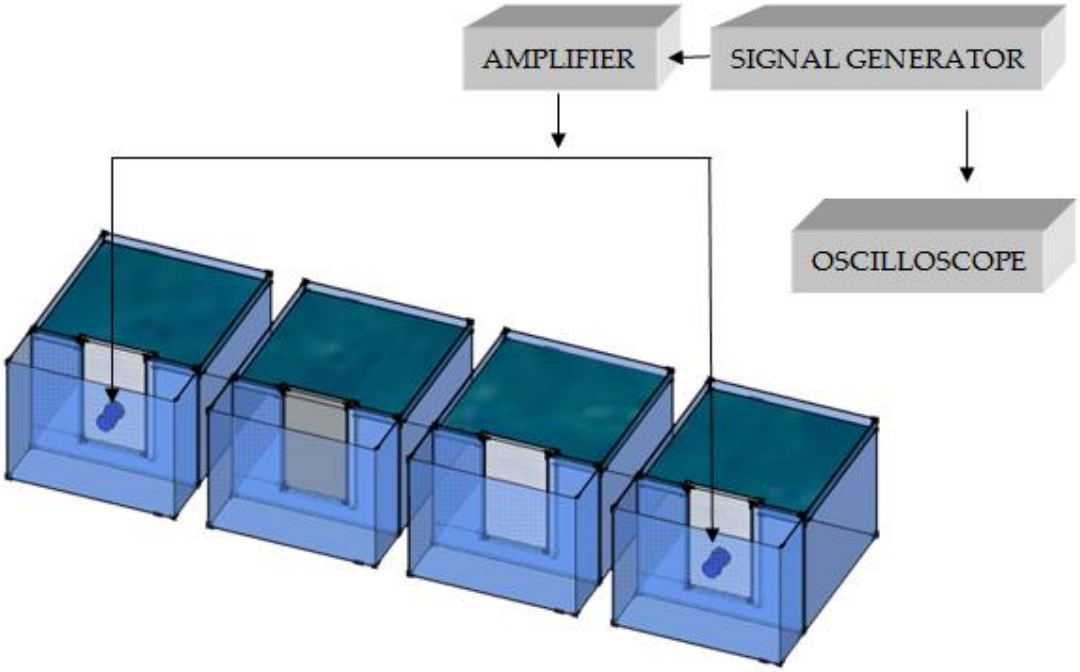

Figure 29. Bioacoustics measurement set up.

The devices shown in figure 29 are listed in the table below:

	Model	Serial number
Signal generator	LEADER LFG – 1310	0100589
Power amplifier	LE 150/025	11199/396
Oscilloscope	HITACHI V212 20 MHz	9284787

Table 5. Acoustical chain used in the completion of the bioacoustics measurement.

	V_{RMS-DC}	V_{RMS-AC}	V_{RMS-AC} VACUO
SINUSOID 20 kHz	108	31.67	75
SWEEP 1st Experiment	75	62	76
SWEEP 2nd Experiment	77	61	76

Table 6. Values measured in parallel to the output of the amplified signal, which feeds to the transducer.

NOTE: Observed voltage drops for sweep signal are only valid as a rough estimation due to the fact that RMS values usually have to be measured on pure sinusoid signals.

Procedure

After having ensured the atmospheric conditions inside the room and once the plates – water – acoustical chain already set up, all the cyprids were mixed on an aside recipient and stir. Next, 5 dl of the solution was inspected under the microscope (twice) to count the average number of cyprids that remained alive after the travel from Tjärno to the measuring facilities. After that, the bulk of cyprids was divided into the four aquariums under salinity – temperature controlled parameters. Data regarding scheduled bio-acoustical measurements are listed in tables 7, 8.

	Date	Cyprids /aquarium	Room temperature	salinity	Light cycle Day : night
1st Trial	20th April 11.30 a.m.	~ 400	15 ºC	15 ‰	8.00:20.00
2nd Trial	11th May 13.30 p.m. 12th May 11.30 p.m.	~ 300 weak Extra ~ 300 Healthy, eager	15 ºC	15 ‰	8.00:20.00

Table 7. Cyprids culture.

	SIGNAL EMITTED	START FREQUENCY	STOP FREQUENCY	TYPE	SYMMETRY	PERIODICITY
1st Trial	Sweep, logarithmic	20 kHz	90 kHz	sinusoidal	off	1 ms
2nd Trial	Sweep, logarithmic	20 kHz	90 kHz	sinusoidal	off	1 ms

Table 8. Acoustical signal emitted.

Electronical performance has been compared to the ultrasonics device commercialized by *Jaycar* [25], CAT. NO. KC5498, which is based on a home-made antifouling ultrasound circuitry kit. This system drives a transducer load of 3 nF with 250 V_{AC}, current drain of 220 mA and supply voltage between 11.5 – 16 V_{MAX}. The characteristics of the emitted signal can be review on their website. The manufacturer states that one unit is enough to cover 32 feet (10 m).

Comparing those values to the ones obtained by measuring with the available acoustic equipment, the signal emitted is less powerful although the measurements take place in aquariums 18 litre big.

Note: it has been observed that when starting the ultrasounds device, some bubbles are produce at the surface of the plate in contact with the water, that is due to gasification process of dissolved oxygen, this may reduce the efficiency of the emitted sound, although those bubbles do not disappear.

Once obtained the first results, several alternatives are considered as changes in the frequency content of the emitted signal or increase of signal amplification. For the last, given to the fact that no other power amplified suitable for this study was available, design and implementation of a home-made amplifier took place.

The analyzed circuit is shown in the next figure 30:

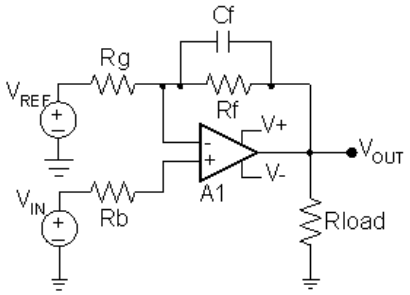

Figure 30 Suggested circuit aimed to drive the ultrasound transducer.

V_{REF}, V_{IN} Voltage reference (usually applied with a continuous supply source) and input voltage to the system, in this situation ultrasonic signal generator.

R_G, R_b Loads at the voltage input.

C_f, R_f Capacitive - resistance load, in this situation it represents the ultrasounds transducer impedance of approximately 3.8 nF.

A1 Operational amplifier model LM717BIN/NOPB. It is a high speed, high frequency working range operational amplifier with flat response until 100 kHz (bandwidth 125 MHz) and fast performance: slew rate 4100 V/μs (voltage ratio change speed).

V_-, V_+ Auxiliary amplifier inputs, supply ∓ 15 VDC, used for stability purposes.

R_{load} Circuit output load, protections against current peaks and oscillation.

The circuit shown above corresponds to a non inverting amplifier, where the output voltage is the amplified input voltage according to a voltage divider:

$$V_{out} = V_{in}\left(1 + \frac{R_f}{R_g}\right) - V_{ref}\left(\frac{R_f}{R_g}\right) \quad (36)$$

For a supply voltage of +-12V and maximum working frequency 200 kHz. If no reference source is connected, gain relies on the relation between resistors. Besides, the capacitor behaves as a low pass filter, attenuation high frequency noise from: $\frac{1}{2\pi}\ C_f, R_f$. The effect obtained with the isolation resistor plus the load capacitor is to increase phase margin in the system by creating a pole and therefore increase stability.

When driving capacitive loads, the previous circuit can be simplified to the following one:

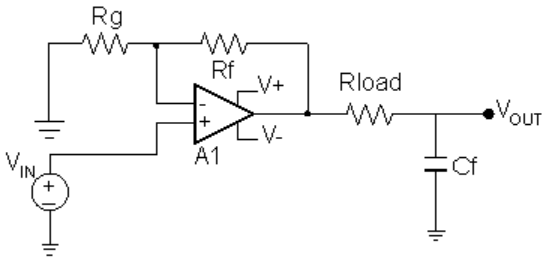

Figure 31 Equivalent circuitry to previous figure 30.

$$V_{out} = V_{in}\left(1 + \frac{R_f}{R_g}\right) \quad (37)$$

According to the manufacturer's instructions, so as to ensure performance stability the

Ratio $V_{out}:V_{in}$ should be similar to 2:1. Once more the capacitor C_f attenuates the high frequency noise as well the resistors give stability to the circuit preventing fast phase variations.

	R_f	R_g	R_{load}	C_f
Units	510 Ω	510 Ω	50 Ω	150 pF

Table 9. Resistance paramaters.

- Frequency signals original equipment ULTRA-10.

So as to get to know how the transducer ULTRA – 10 works, a preliminary study of its frequency response was carried out in the next figure.

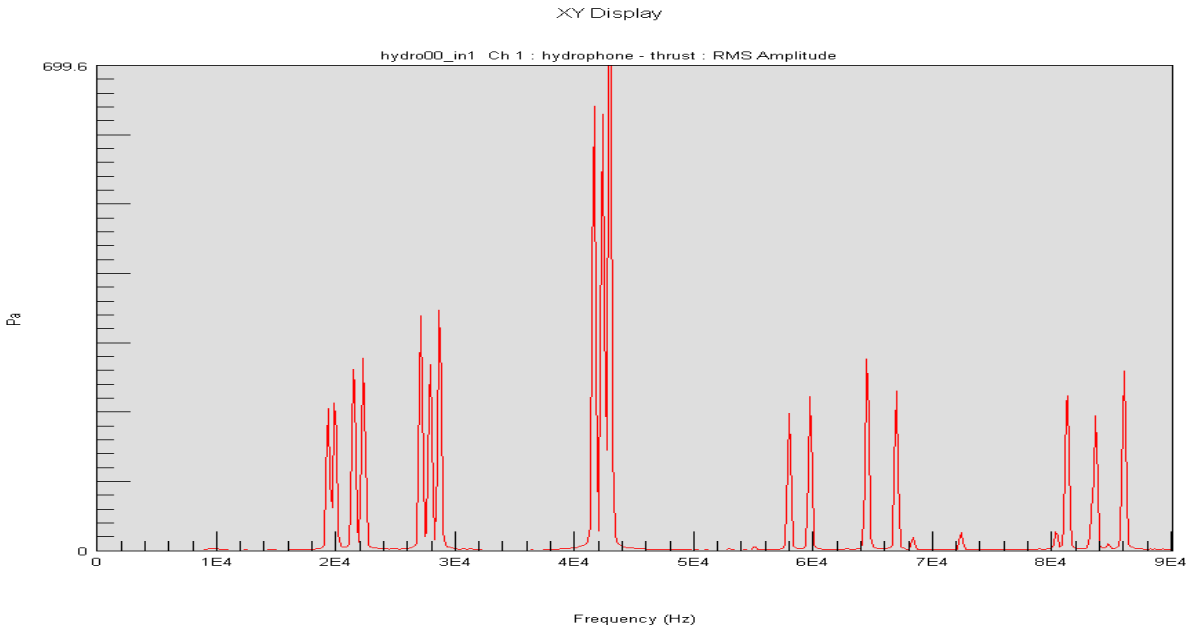

Figure 32. Main energy distribution in frequency. In the figure it can be seen that the major pressure is sent close to the transducer resonance (40 kHz).

The previous figure 32 shows that there is a major resonance at the transducer performance around 40 kHz. This data has to be taken into account to excite the transducer easily.

The simulation of the 1st trial signal has been carried out with MATLAB ("signal 1"), it is a logarithmic sweep similar to the one set up in the signal generator. Its properties are:

$$f_i(t) = f_0\,\beta^t$$

$$\beta = (f_1/f_0)^{1/t_1} \qquad (38)$$

$f_i(t)$, f_0 Sweep frequency output at time t; sweep starting frequency corresponding to t0

β^t Time increment.

Quadratic sweep (signal 2) has also been observed, it can be generated as follows:

$$f_i(t) = f_0 + \beta t^2$$

$$\beta = (f_1 - f_0)/t_1^2 \qquad (39)$$

$f_1 - f_0$ stand for final frequency – initial frequency for the sweep.

Where (t_1 - t_0) is the signal period; resolution 1ms equivalent to 1 kHz.

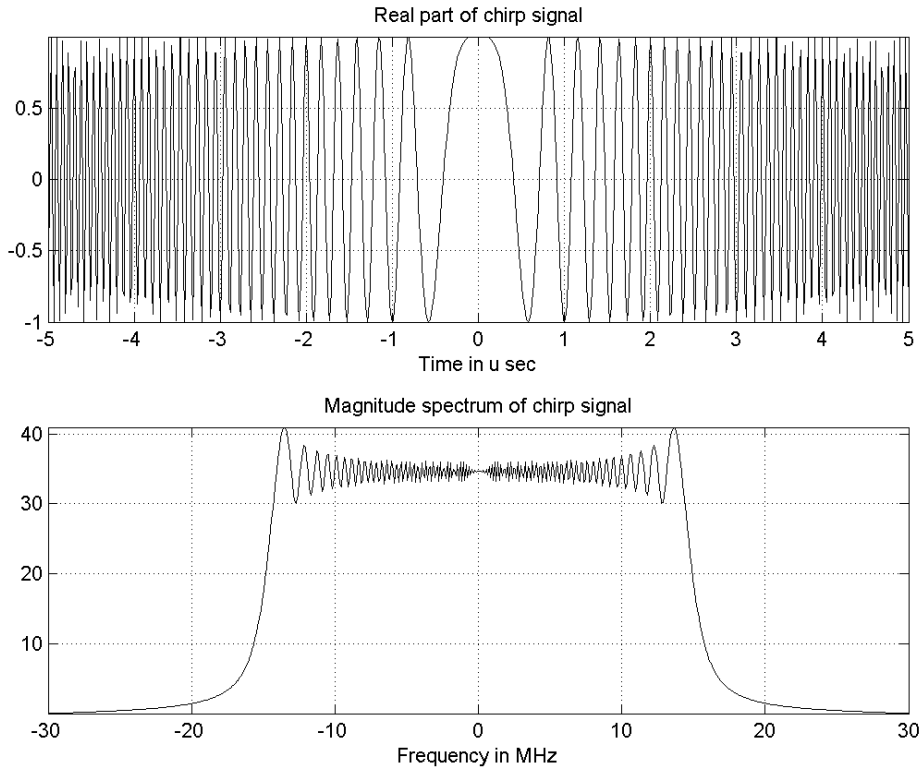

Figure 33 Example of a high frequency chirp in the Programmers United Develop net [25].

In order to optimize the emitted signal so as to radiate the most, sinusoidal and quadratic sweeps have been considered and analyzed through their power spectra. Thus, the following figure 34 shows the energy distribution on both situations:

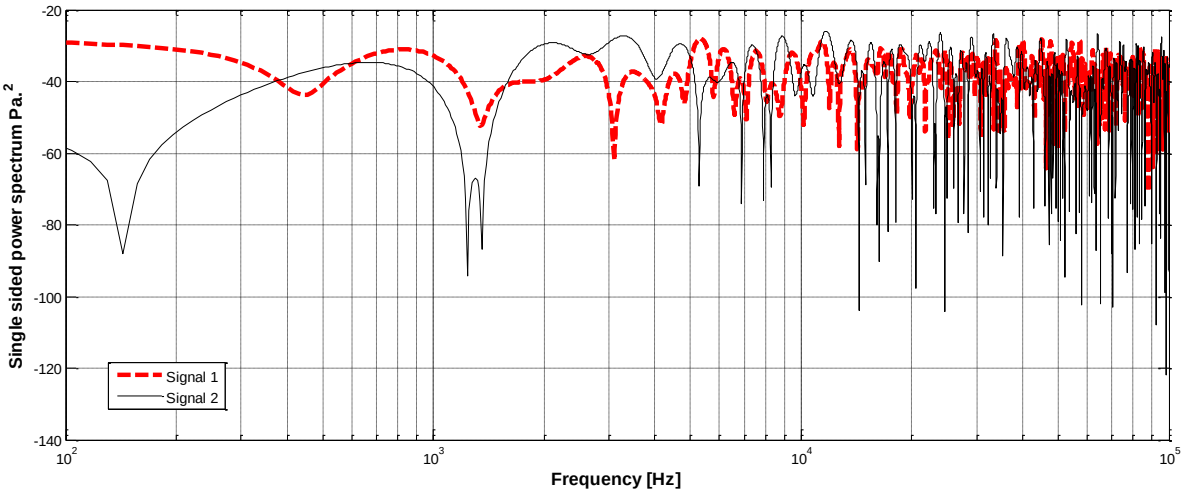

Figure 34. Sound power density comparison: signal 1 – signal 2 correspond to sinusoidal – quadratic sweep shape. As it can be seen at the aimed frequency range (20 kHz to 90 kHz), emission of either kind of sweep gives no huge differences

	f_0	f_1	t
Units	30 kHz	90 kHz	1s

Table 10. Values used to obtained the signals of figure 34..

4.2 Bio- acoustics experiments

The results obtained from the first measurement round were collected the 2nd May at 13.15 p.m., thus 12 days of culture under controlled environment. For the second round (starting 11th May) the same methodology was applied.

4.2.1 Conclusions first round

The aquariums labels are as follows:

			FIRST ROUND	
	Acoustic device	**Plate**	**Data 1**	**Data2**
Aquarium 1	✓	Aluminium	26.3 %	51.9 %
Aquarium 2	No	Aluminium	50.7 %	100 %
Aquarium 3	No	Plexiglas	100 %	200 %
Aquarium 4	✓	Aluminium Plexiglas	21.2 %	41.8%

Table 11. Biological results 1st measurement round. The percentages are relative to the aquarium marked as 100 %.

Note: Data 1 Culture referred to Aquarium 3, only plexiglass plate.

Data 2 Culture referred to Aquarium 2, only aluminium plate.

Note that the phenomena observed on Aquarium 1, second round referred to aquarium 2: column "Data 2" is explained in the further section 4.2.3 diagram 2.

Culture success: beginning ~ 400 Reference aquarium 3 ~ 254 → 63.5 %

To sum up, relative to the initial amount of larvae at the beginning of the experiment, using data from aquarium 3, the culture success is 63.5 %.

Regarding the acoustical chain at the end of the culture, levels and set up have been checked to ensure same performance as at the beginning of the measurement.

In relation to the biological behaviour: plates were removed from the aquariums and kept in optimal water conditions. The organisms were counted and divided in two categories:

(1) Cyprids: organisms that are attached to the plate but have not started the transformation process.

(2) Balanus: organisms that have finished metamorphosis, already feeding from water nutrients.

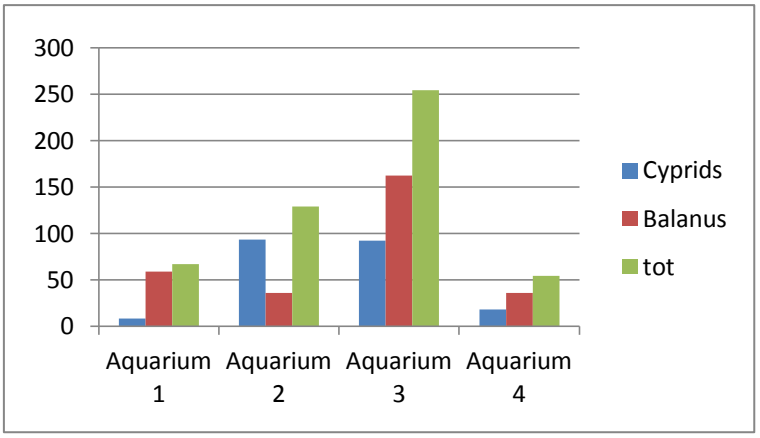

Diagram 1 Bio acoustical culture results after first round.

Case aquarium 4: apart from the results in number it has been observed that in the Plexiglas plate placed in front of the aluminum plate, the proportional number of organisms is considerably less than in aquarium 3, in that situation the equipment was placed as follows:

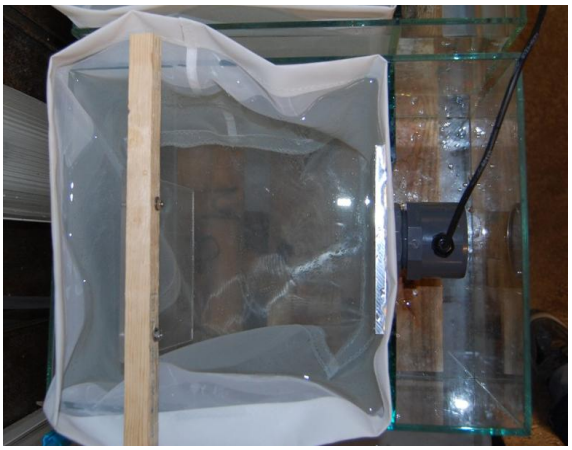

Figure 35 Upper view of aquarium 4. Right hand side ultrasounds transducer attached to the aluminium plate, left hand side hanging plexiglass plate from a wooden piece.

- Study of sound propagation and damping first order reflections

Nets observation

Aquarium 1: Overall number about 20 individuals distributed spread between waterline and corners. Many organisms observed on the bottom. Note: this population also known as NET_REF.

Aquarium 2: Population of approximately 5 times NET_REF, distributed along waterline and corners.

Aquarium 3: Population double as NET_REF concentrated along waterline.

Aquarium 4: 2.5 times NET_REF, locally placed at the furthest corner from the applied sound, waterline.

General observance

The general tendency in those aquariums containing aluminium plates with sound device on the total number of individuals in low. Besides, comparing aquarium 1, 4 in the latest the cyprids took shelter behind the test movable Plexiglas plate, locally at the corners. Little population found on the net placed inside aquarium 3 due to the fact that the attachment success was high.

4.2.2 Conclusions second experiments round

The following table 11b, summarizes the results obtained in the second biological measurement round:

			SECOND ROUND	
	Acoustic device	**Plate**	**Data1**	**Data 2**
Aquarium 2	No	Aluminium	71 %	100%
Aquarium 3	No	Plexiglas	100%	140%
Aquarium 4	✓	Aluminium Plexiglas	47%	60 %

Table 11b. Biological results 2nd measurement round. The percentages are relative to the aquarium marked as 100 %.

Note: Data 1 Culture referred to Aquarium 3, only plexiglass plate.

Data 2 Culture referred to Aquarium 2, only aluminium plate.

Note that in the second round, the results observed in the aquarium number 1 should not be considered given inaccuracies accounted during the beginning of the measurement. The amount of larvae placed in this aquarium was higher than in the other aquariums (explanation table 7, placement of larvae 11 th – 12th May 2011), fact that polluted the results of aquarium 1. This effect is shown in the next diagram 2:

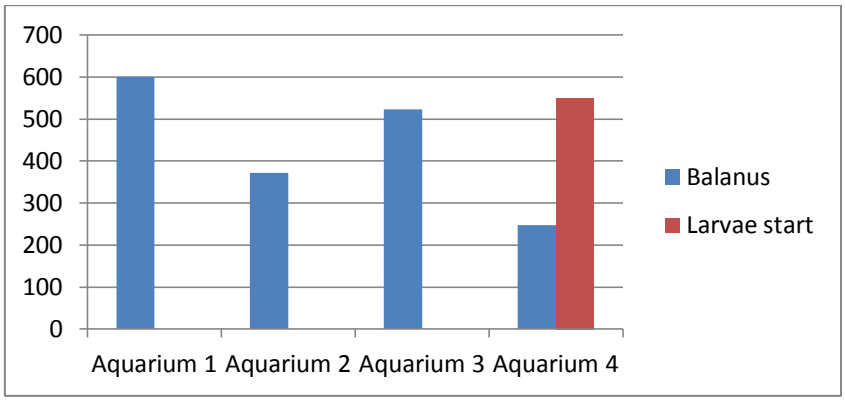

Diagram 2. Amount of barnacles counted in each aquarium.

As referred in Table 11b, the explanation for the culture obtained in Aquarium 1 remains unknown (counted a higher number of balanus at the end of the experiment than supposed number of larvae at the beginning) but it can due to a misdistribution of the larvae at the beginning of the experiment round 2.

General observance

During the whole measurement, acoustic and environmental conditions were checked following the procedure of the previous round to neglect differences in acoustic power at the beginning – end of the measurement and therefore effects in environmental changes. The only difference between both measurements relays on the fact that for first round the surface of the aluminium plates remained unpainted while in the second round a primer painting has been applied on the plates. This primer in antifouling free and represents a surface that the cyprids are found of.

Taking into account that the starting amount of larvae before the measurement began it was considered to be around 500 ~ 600 and the balanus counted in one of the aquariums is more than at the theoretical start, it is clear that the distribution has been uneven inside the aquariums and that the amount of organisms at the beginning of this culture remains unknown.

Despite of the results in aquarium No. 1, when comparing the effect of the acoustic device in aquarium 4 and aquarium 2, it can be seen that the acoustic approach has an effect in the culture observed on the plate although the data show that this measurement should be repeated so as to ensure the results from the first measurement round.

Differences in the animal morphology between both measurements are noticeable given that in the second measurement round all the organisms counted had already approached metamorphosis stage and no cyprids were seen but only juvenile balanus, as it can be observed in the next figure:

Figure 36. Averaged balanoids morphology observed on the organisms attached at the plates at the second measurement round.

Although it is difficult to see, the animal has accomplished first metamorphosis stage –juvenile barnacle. This fact is determined by auto-feeding behaviour: the middle line that cross its body ("egg shaped") delimits two movable shell plates (explained already in picture 2) used to catch nutrients from the water, besides, the small lines around its shape could be the feeding leg in motion so as to scan the water close to the animal (low photography shutter speed: in this picture all the surrounding legs could be visual superposition of the unique one in long photographic exposure time).

4.3 Radiation

4.3.1 Study of propagated waves inside the material.

After having carried put the mathematics analysis described in part 3. 4, the lower frequency limit applied is set up to 20 kHz. The plate mechanic's characteristics are shown in Appendix C.

The calculations according to the MPT, lead to the fact that the compressional wave is the predominant given that they travel longer distance, thus for a 1 cm thick aluminium plate, the waves propagated through the material have the following wavelengths:

	Compressional	Shear	Flexural	Rayleigh
Wavelengths	27 cm	15 cm	7 cm	12.7 cm

Table 12. Calculated wvalengths according to equation (7) for a frequency f = 20 kHz.

Calculations on table 12 based on the theory of part 3.1 as well as the mechanical properties of the aluminium Appendix C. The calculation of the flexural wavelength has been done for 20 kHz.

As a consequence of the previous estimations, the radiation effects are mostly based on compressional waves. In order to adequate the numerical models based on infinite plates with real measurements, avoid reflections from the edges leading to the relation wave number being much smaller compared to the dimensions of the plate. Theoretical requirements: finite plates, neglect reflections from edges by fixing wavelengths smaller than dimensions; applied harmonic point force.

As it is detailed in the next parts, the radiation measurements were accomplished on two plates with different sizes though same mechanic properties – thickness. First measurements carried out with the aluminium plates used previously in the biological measurements, given their size, study at 80 kHz (compressional wavelength 7.5 cm). Second measurements carried out with a bigger plate to contain few wave lengths along its geometry. While observing radiation pattern in the plate, it was hanged so as to avoid coupling effects with adjacent structures.

Expected cylindrical spreading: $A \propto 1/\sqrt{r}$

A Wave's pressure amplitude [Pa]

r distance [m]

4.3.2 Transducers set up – acoustical supply chain

According to the measured values on the real set up, the signal amplitude for all the theoretical studies has been 212 volts peak to peak, equivalent to 75 V_{RMS}.

The collected data corresponds to averaged values over 10 s.

Measurement equipment:

	Type	Serial No.	Sensibility	Range
Acc.1. Channel 1	352A60 PCB	123037	1.073 mV/m/s^2	1000 mV
Acc.2. Channel 2	352A60 PCB	123038	1.047 mV/m/s^2	1000 mV
Hydrophone	8103 B&K	1375176	101 e^{-3} pC /Pa	10 V

Table 13. Transducers set up.

- Charge amplifier Type 2635 B&K, AB VOLVO PENTA 000658
- Acquisition system DEWETRON 2014, AB VOLVO PENTA DEWE 43, set up:

	Sampling frequency	Number of samples	Bias	High Pass
Value	200 kHz	40000	11 V	10 Hz

Table 14. Acquisition system set up.

4.3.3 First radiation measurement – plate A.

A first round of radiation throughout the aluminium plate took place. In that situation the plate used was the same as the one located inside the aquarium when accomplishing the bioacoustics measurements.

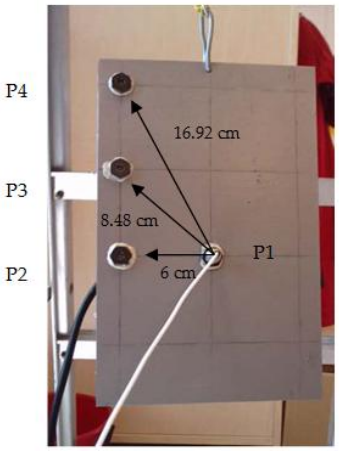

	P1	P2	P3	P4	P5
Length	0	6	6	12	6
Width	0	0	0	0	-0.08
Height	0	0	6	6	0

Table 15. Measurement points plate A. Dimensions figure 22.

Figure 37. Aluminium Plate A. Table 13 shows the measurements points in which point P5 in the plate corresponds to the P2 in the back side (close to the transducer).

4.3.4 Second radiation measurement – plate B.

Once processing the results obtained from the measurement in plate A, the same measurements took place in a bigger plate to be able to get a better understanding on the acoustic excitation of the plate and the similitude of the real damping and theoretical (water load).

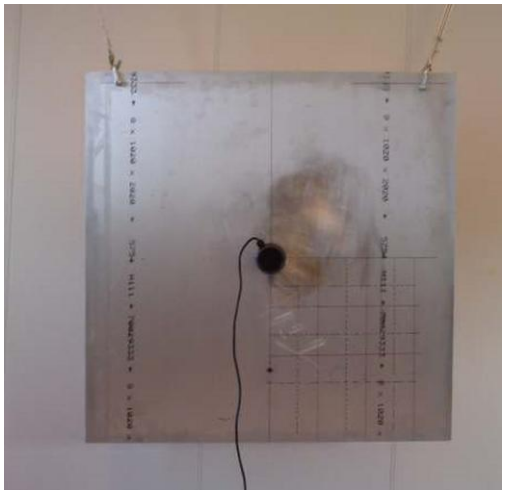

Figure 38. Aluminium Plate B. Dimensions 100 x 100 cm. Thickness 1 cm.

	P1	P2	P3	P4	P5
Length	0	6	6	12	6
Width	0	0	0	0	-0.08
Height	0	0	6	6	0

Table 16. Measuring points plate B

4.3.5 Underwater propagation – aquariums.

The set up for the noise studies inside the aquarium is as follows:

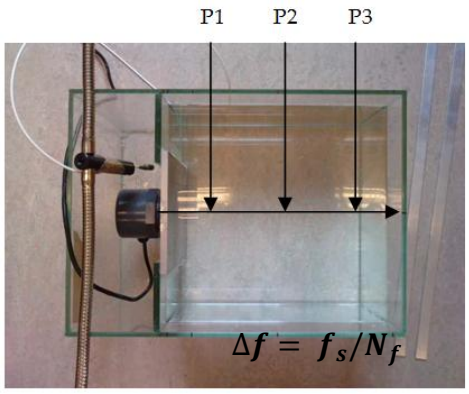

Figure 39. Sound pressure measurements points inside the aquarium

	P1	P2	P3	Airborne
Length	4 cm	14 cm	28 cm	-2 cm
Width	0	0	0	+3 cm
Height	14 cm	14 cm	14 cm	14 cm

Table 17. Measurement points in the aquarium, considering origin aligned with mid- plane of the UT transducer.

Next table shows the acquisition system – signal processing properties for the radiation measurements.

	Sampling frequency	Block size	Δf	
Acquisition	200 kHz	40000	5 Hz	
FFT Analysis	200 kHz	32768	6.10 Hz	Hanning window, 67 % overlap

Table 18. Acquisition system set up.

4.3.6 Vibration results – Plate A

The following test was carried out in order to evaluate for different exciting frequencies, the frequency range at which the plate radiates better:

Excitation Frequency	**2 kHz**		**8 kHz**		**80 kHz**	
Strongest resonance	39746 Hz		39941 Hz		80664	
	Acceleration [m/s^2]	Velocity [m/s]	Acceleration [m/s^2]	Velocity [m/s]	Acceleration [m/s^2]	Velocity [m/s]
Point 2	4.93	1.97 e-005	78	3.10 e-004	260	5.13 e-004
Point 5	12.65	5.06 e-005	217	8.64 e-004	117	2.30 e-004

Table 19. Recorded signals Plate A.

It can be seen that when exciting at frequencies below the transducer resonance frequency, still this resonance emits almost all the energy through the plate. Thus, a sweep in frequency from 0.1 to 10 kHz was performed, the results showed that it has been noticeable that the higher response was obtained when exciting the transducer close to its resonance frequency. This preliminary study motivated a deeper analysis on the plate response at both 40 kHz and 80 kHz.

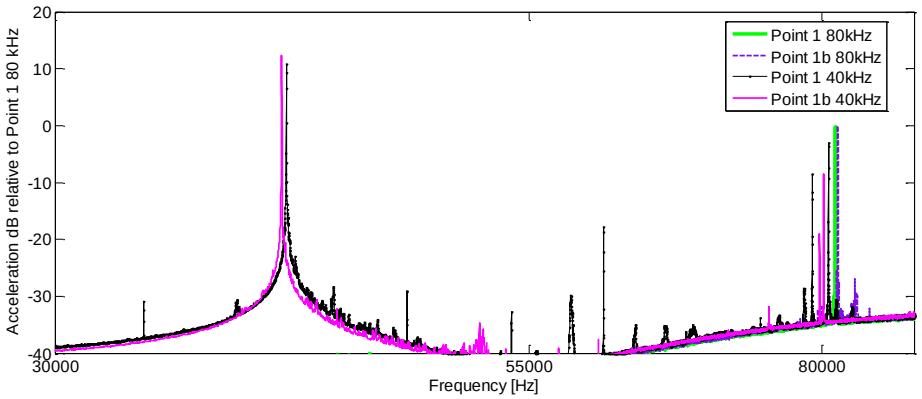

Figure 40. Acceleration recorded at different measured points on the plate.

The above plot shows the response of the plate through the thickness when the exciting frequencies are 40 kHz and 80 kHz. As it can be seen when normalizing the response in reference to point 1 at 80 kHz, the levels obtained when exciting at 40 kHz are higher.

	Measured 80 kHz		Measured 40 kHz		**Theoretical water load 80 / 40 kHz**	**Theoretical air load 80/ 40 kHz**
	Acceleration [m/s^2]	**Velocity [m/s]**	**Acceleration [m/s]**	**Velocity [m/s]**	**Velocity [m/s]**	**Velocity [m/s]**
Point 1	181.80	3.61 e-4	886	35 e-3	MAX	MAX
Point 2	86.95	1.72 e-4	713.8	28 e-3	3.49 e-5/ 3.49 e-5	27 e-3/ 27.07 e-3
Point 3	151.10	3.00 e-4	213	6.01 e-4	2.57 e-5/ 2.56 e-5	18.6 e-3/ 18.6 e-3
Point 4	78.74	1.56 e-4	420	3.13 e-4	1.40 e-5/ 1.49 e-5	1.7 e-4/ 1.9 e-4

Table 20. Recorded data plate A at points 1 -4.

4.3.7 Vibration results – Plate B

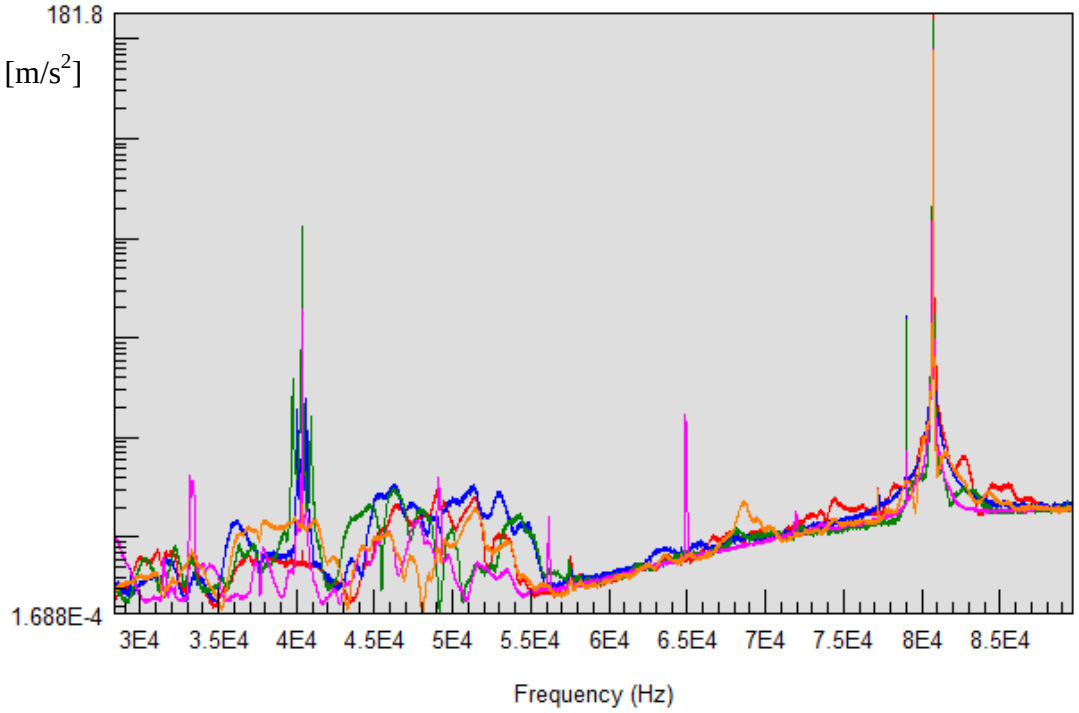

Figure 41. Measured acceleration values for small plate (y- axis). Excitation frequency 80 kHz.

Besides, during the acoustic system inspection it has been noticeable that the influence of the transducer response is much bigger than the material properties, thus first of all a sinusoidal sweep from 0-1 – 10 kHz took place in order to identify the most important frequencies leading to measurements applying point excitation force of 40 kHz – 80 kHz. The results for different points close to the device are shown in the next figures. Note that plate symmetry has been considered in length – height.

A second evaluation of the wave response on a bigger plate took place in order to ensure the application of the infinite plates theory for the study case and after having performed a sweep from 20 – 90 kHz as the transducer resonance has a bigger impact on the radiated energy, a second measurement was carried out exciting the plate at 40 kHz.

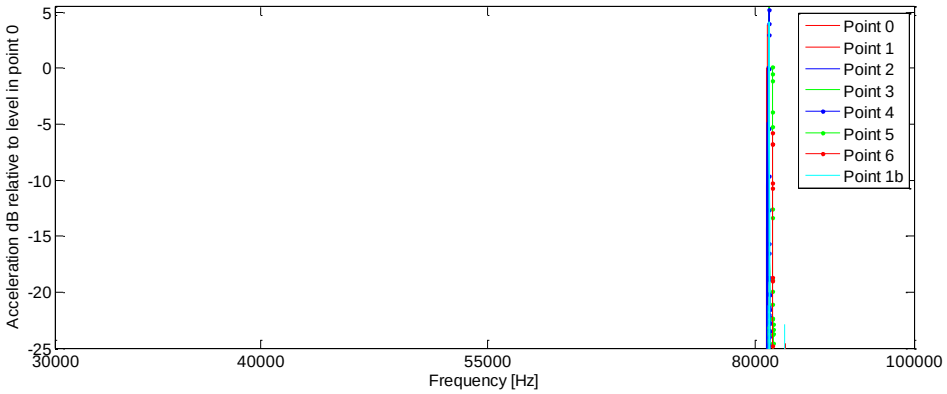

Figure 42. Acceleration at each measured point relative to point 0: excitation point other side of the plate. Excitation frequency 80 kHz.

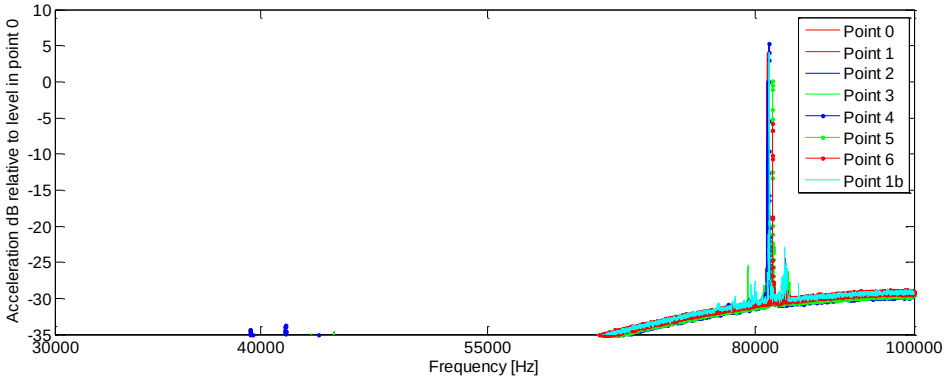

Figure 43. Results acceleration at each measured point relative to point 0, bigger dynamic range. Excitation frequency 80 kHz.

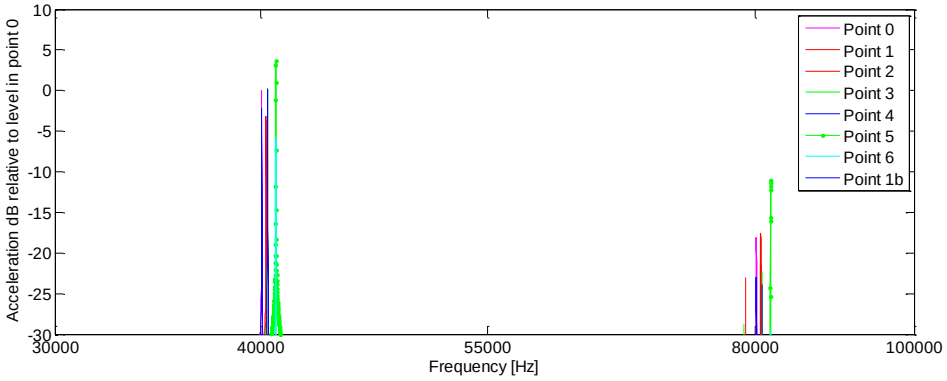

Figure 44. Acceleration at each measured point relative to point 0. Excitation frequency 40 kHz.

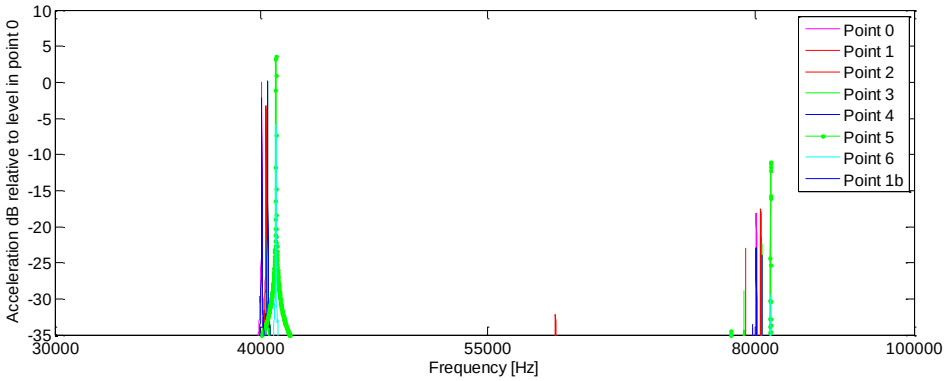

Figure 45. Results acceleration at each measured point relative to point 0, bigger dynamic range. Excitation frequency 40 kHz.

During the measurement on the response of the plate, it was hanged but no extra damping was added. A deeper look at the materials properties has shown that the losses of the plate when no painting or extra material layers are applied are negligible, thus no infinite theory can be applied. This fact explains the results obtained in several measurement points when the amplitude tendency –decreasing levels with increasing distance- do not follow the expected trend. Therefore, the losses [dB] in distance for the given situation is as follows:

$$Material\ losses = 20\log\left(e^{-\frac{\eta}{4}x}\right) \qquad (40)$$

In order to adequate this situation with the numerical analysis extra damping should have been applied, or else the measurements should have taken place with water load on one side of the plate, case not feasible in reality given the lack of waterproof accelerometers.

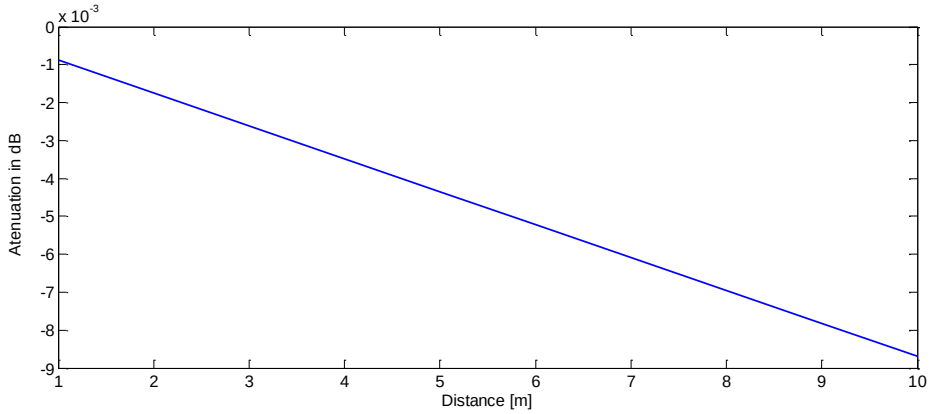

Figure 46. Losses of alumminium plate, Appendix C. Losses η=0,1%.

4.3.8 Sound propagation – dissipation in the aquarium.

The data shown in the above plot corresponds to average pressure in the aquarium during 40 s when the sweep according to the biological measurements was played.

	Position 1	Position 2	Position 3
Pressure Pa	1096	1074	922.1
dB re 1µPa	180.8	180.6	179.2

Table 20. Average pressure in the aquariums.

No noticeable attenuation from middle to the end of the aquarium was observed.

5 Conclusions & future work

5.1 Biological experiments

Regarding the biological measurements, the first measurement round was satisfactory whereas the second round was not that successful, although in both situations there can be seen obvious effect on the organisms response towards the sound. After having collected the results from the second round of experiments one of the conclusions could be that the organisms distribution was not completely under controlled. This phenomenon can be explained due to the fact that the cyprids were placed inside the aquariums in two consecutive days which increases the risk of uneven distribution. Besides, the animals belonged to two cultures in slightly different growth phase. For future work a new routine has to be established based on double check: counting the amount of living organisms before placing them inside each aquarium (done in both experiments) as well as taking samples of the tanks after having introduced them .This way the initial quantity of cyprids on each aquarium may be better estimated.

Furthermore, the cyprids should be used at their arrival at the measuring facilities, avoiding organisms to weaken or already start the metamorphosis process before applying the sound. Although I tried to make sure of this good timing while planning the experiments, coordination of the different suppliers has been tedious. To sum up, there is a obvious disturbance in the animal behaviour when ultrasound is applied on the plate that should be further examined.

To ensure stability regarding electrical supply during the bio –acoustics experiments (few days /24 hours non - stop). The power input – output was verified to be the same at the beginning – end of the measurement.

5.2 Radiation measurements

In accordance to the radiation measurements, it is noticeable that the theoretical consideration on infinite plates has not been fulfilled. This matter complicates the comparison between theory and reality making it difficult to estimate the accuracy of the numerical analysis. As explained in the results chapter, the losses of pure aluminium are negligible for the given plates, thus there exists a high risk in placing the accelerometers at positions where the energy is concentrated. Therefore, the results may show no tendency in decreasing particle displacement for increasing propagation distances, which ideally should follow spherical propagation. In the first observances on the small plate the results look more coherent to theory, whereas the data obtained after measuring the big plate remain doubtful. So as to avoid such effect, either a damping layer should be glued to the plate to resemble the water load or the plate should be introduced in a big tank of water. In the case of damping layer applied its properties can be analyzed with LLW (Leaky Lamb Waves) order zero so that it resembles water load.

Nevertheless, although the experiments do not bring understandable numbers, they show clear conclusions on the material radiation concerning frequency range. This knowledge can be very useful for next experiments to improve power radiated towards the water.

Moreover, the acquisition system used has limited accuracy for ultrasonic frequencies in respect of number of samples, fact that decreases the chances of obtaining valuable data. Also, it would be good to have the possibility of using ultrasonic waterproof accelerometers to check particle velocity in the water. Furthermore, given the results of the electrical measurements on the transducer, in the case of using the ultrasound transducer on a real hull, a specific amplifier for ultrasonic frequencies should be in use.

To conclude, after carrying out those measurements, results show that this approach works although more test should be carried out as well as adjust the frequency range at the optimal frequency range according to the radiation measurements.

6 Bibliography

[1] Dennington Simon: Understanding Marine Fouling and Assessing Antifouling Approaches, National Centre for Advanced Tribology at Southampton (Ncats), School of Engineering Sciences, University of Southampton.

[2] Woods Hole Oceanographic Institute (1952): Factors Influencing the Attachment and adherence of Fouling Organisms, Woods Hole Oceanographic Institute. No.580. Copyright 1952 by US. Naval Institute, Annapolis Maryland George Banta Publishing co. Menasha WI.

[3] [Matz B] states for conclusions after meeting with Matz Berggren at the Kristinebergs Test Centre.

[4] Khandeparker, Lidita, Chandrashekhar Anil, Arga: Underwater adhesion: the barnacle way, Publication code 403-004, National Institute of Oceanography, Dona Paula, Goa.

[5] Karl Tate (December 2006): Kyprogenesis.

Accessible at:

http://kypria.blogspot.com/2008/05/bibiki-persian-for-goose-barnacle.html

[6] Visscher J. P. BioI. Bull.(1928): Reactions of the Cyprid Larvae of Barnacles at the Time of Attachment, Visscher J. P. BioI. Bull. Biological Bulletin Vol 54, No. 4 327-335. 1928.

[7] Dürr, Simone, C. Thomason Jeremy: Biofouling: ISBN 978-1-4051-6926-4

[8] European Network of invasive species (barnacles' distribution in different seashores) Accessible at:

http://www.nobanis.org/speciesInfo.asp?taxaID=255

[9] C. Junger Miguel, Feit David (1986): Sound, Structures and Their Interaction. Cambridge, MA, MIT Press, 1986, 460 p.

[10] American Boat & Yacht Council Accessible at:

http://www.ndt-ed.org/

[11] Hannsen Su, J., Vasudevan, R. (1997): On the Radiation efficiency of infinite plates subject to a point load in water, Journal of Sound and Vibration, Volume 208, Issue 3, 4 December 1997, Pages 441‑455

[12] Dr. Jessey. California Polytechnic University-Pomona Geological Sciences Department. Accessible at:
http://geology.csupomona.edu/drjessey/class/Gsc101/Earthquake.html

[13] Dr. Kropp, Wolfgang (2010): Notes of Technical Acoustics 1, Applied Acoustics Division Chalmers University of Technology, Gothenburg, Sweden.

[14] Stephen, N.G. (1997): Mindlin Plate Theory: Best shear coefficient and higher spectra validity. Journal of Sound and Vibration Vol. 202, Issue 4, 15 May 1997 Pages 539 – 553.

[15] K. M. Liew Y. xiang, S. Kitipornchai and J.L Meek (1993): Formulation of Mindlin – Engesser model for stiffened plate vibration, Computer Methods in Applied Mechanics and Engineering Vol. 120, issues 3-4, February 1995, pages 339 – 353.

[16] Stephen, N.G. (1997): Mindlin Plate Theory: Best shear coefficient and higher spectra validity. Journal of Sound and Vibration Vol. 202, Issue 4, 15 May 1997 Pages 539 – 553.

[17] R. A. Apakashev and V. V. Pavlov (1997): Determination of the shear strength and modulus of water at low flow velocities. Fluid Dynamics Volume 32, Number 1, 1-4, DOI: 10.1007/BF02697929

[18] Kuttruff, Heinrich, (1991): Ultrasonics: fundamentals and applications. London, Elsevier Applied Science, 1991 058073418

[19] Emmanuel C. Ifeachor. (1988):Digital Signal Processing. Publisher Person Educated Limited (1993-2002) , ISBN-13: 978-0-201-59619-9.

[20] Todd. F.H. (1961): Ship Hull Vibration, Open library OL20013353M

[21] Spiros Kotopoulis, Antje Schommartz & Michiel Postemal: Sonic cracking of blue-green algae. Applied acoustics volume 70 number 10 ISSN 0003-682X, October 2009.

[22] Marin Akustikk, course notes at NTNU 2010.

[23] Bostik website, accessible at:

www.bostik.se

[24] Flexidal Technics website, accessible at:

http://flexidal.be/

[25] Jaycar Electronics website, accessible at:

http://www.jaycar.com.au/

[26] Davies, B (1984): Integral Transforms and Their Applications, 2nd ed., Springer-Verlag, New York, 1984. ISBN: 0-387-95314-0.

Appendix A. Hankel Transform

According to *Davies B* [26], zero order Hankel transform can be seen as 2- D Fourier – Bessel transform, it defines a function as a sum of infinite Bessel functions of first kind can be Explanation (γ) plane

- Hankel transform $F_v(k) = \int_0^\infty f(r) J_v(kr) r\, dr$ (41)
- Inverse Hankel transform $f(r) = \int_0^\infty F_v(k) v(kr) k\, dk$ (42)

For f(r), $J_v(kr)$, v function, Bessel functions first kind and order respectively. For a detailed explanation on Hankel transforms and its relationship with Fourier transforms, read Operational and convolution properties of two- dimensional Fourier transforms.

- Calculation gamma values:

Hankel transforms are applied in studies under radial symmetry. Thus, according to Mindlin model "Thick plate theory", reference *N. G. Stephen* [16], the transform wavenumbers γ, that show the relationship between pressure – particle displacement at the boundary plane z=0 are obtained by solving the following polynomial:

$$\gamma^{10} - (k^2 + 2k_s^2)\gamma^8 + (k_s^4 + \tau^4 + 2k^2k_s^2)\gamma^6 - (2\tau^4(k^2 + k_s^2) + k^2k_s^4 + R)\gamma^4 + (\tau^8 + 2k^2k_s^2\tau^4 - 2\aleph R)\gamma^2 - (k^2\tau^8 + \aleph^2 R) = 0 \quad (43)$$

Where:

$k_s^2 = k_c^2 + k_R^2$ (44)

k_C, k_R corresponding to k in medium and c_R explained in part 3.1

$k_m^4 = k_c^2 k_R^2$ (45)

$\tau^4 = k_m^4 - k_c^4$ (46)

$R = \left[\left(\frac{h^2}{12}\right)\left(\frac{k_R}{k_c}\right)^2\right]\rho^2 k_f^8/m^2$ (47)

m is the mass [kg], h thickness [m], k_f flexural wavenumber [m^{-1}] explained part 3.2

$\aleph = \left(\left(\frac{12}{h^2 k_R^2}\right) - 1\right)k_c^2$ (48)

Asymptotic form to calculate Hankel function order n

$$H_n(x) = \sqrt{\frac{2}{\pi x}}\,(-i)^n e^{(ix - i\pi/4)} \quad x \gg n^2 + 1 \quad (49)$$

Order 0, with $x = \gamma r$

- Contour of integration $Re\left(\sqrt{\gamma^2 - k^2}\right) > 0$ if observing poles in the low limit for frequencies that accomplish $\frac{\omega}{\omega_c} \ll 1$ for ω_c

$$\gamma = k_f\left[1 + \frac{\varepsilon}{\sqrt{\Omega(1-\Omega)}}\right]^{1/4} \quad (50)$$

$$\varepsilon = \frac{\rho c}{\omega \rho_s h} \qquad (51)$$ Fluid loading at any frequency

Where γ are the residues obtained by applying Cauchy over the contour C.

The inverse Hankel transform can be solved as the integral over the branch cut plus the residues in the positive γ plane, known as the method of stationary phase.

As seen before, there are different waves generated, those which phase (γ) varies slowly are the ones with major contribution. Yields, equivalent to solve the integral for the three real waves generated, minding the existence of a real pole that can be avoided by introducing material damping, η_s, as:

$$E = E(1 - i\eta_s) \qquad (52)$$

E material's Young Modulus [GPa]

For far field

- k·fr >>1, the contribution of the residues n = 2,3, … is negligible, thus calculations can be carried out applying:

$$\gamma \approx \gamma_1 = k_f(\rho/\rho_s k_f h)^{1/5} \qquad (53)$$

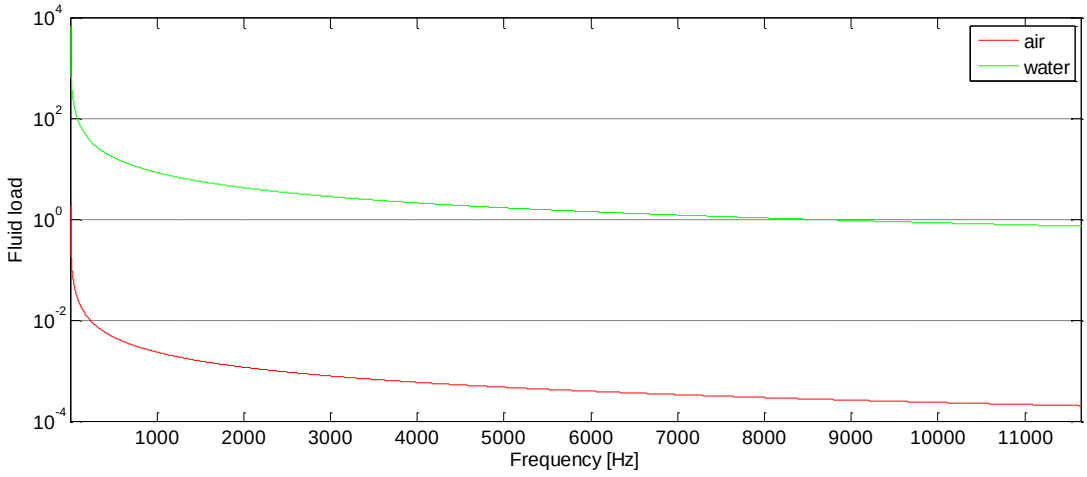

Figure 47. Fluid load for air and water.

Appendix B. Fiberglass behaviour

Next, waves analyzed in fiberglass plates with numerical models.

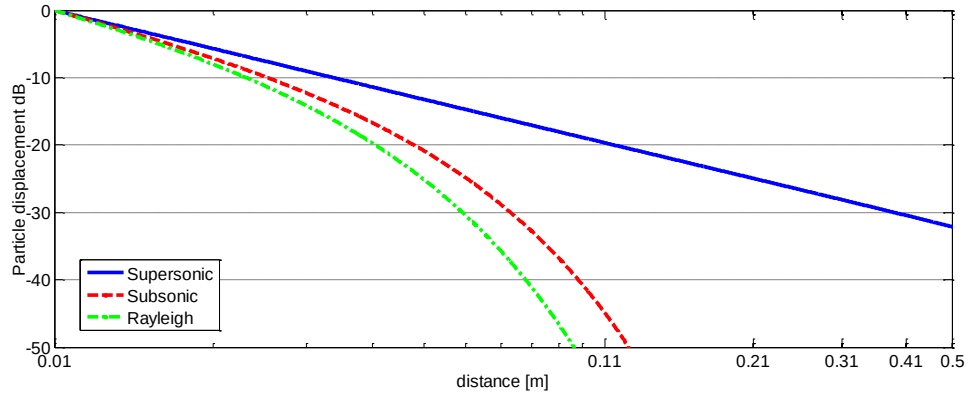

Figure 48 Particle displacement relative to amplitude at 1 cm distance, similar to aluminium case

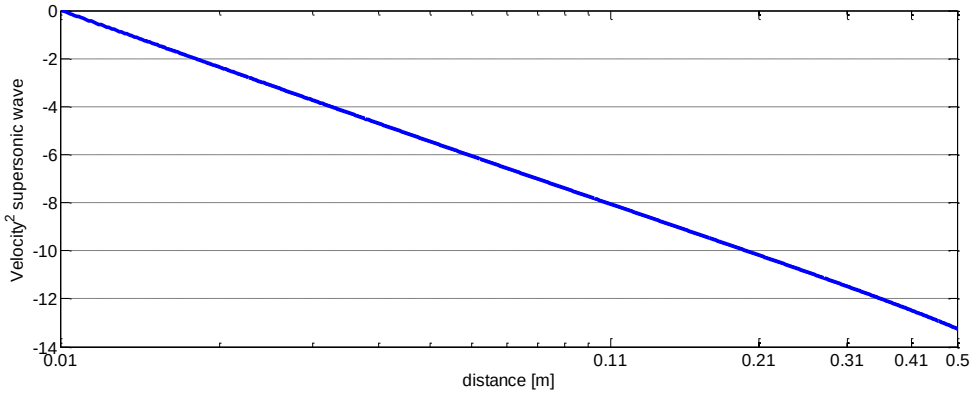

Figure 49. Squared velocity - high frequency model - relative to amplitude at 1 cm distance. Comparing this figure with figure 3, in the situation of aluminium the velocity decreases faster with fiberglass, though the difference is not large.

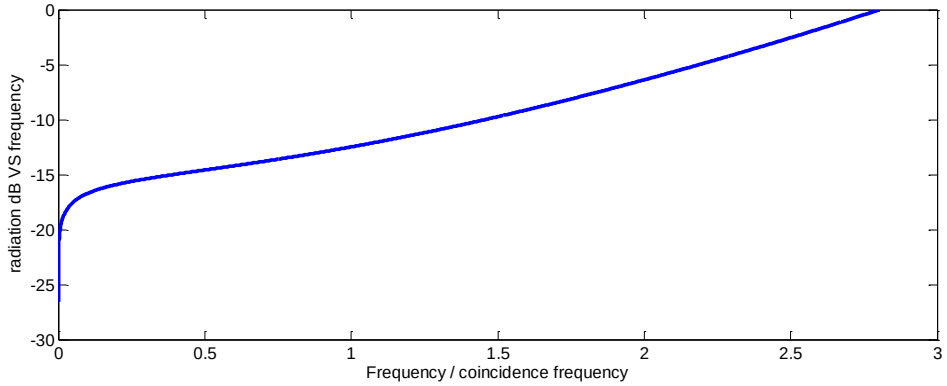

Figure 50. Radiation efficiency fiberglass. When comparing this curve with the one obtained for aluminium plates (figure 19), it can be observed that the slope is increasing slightly faster thus achieving 0 dB (value =1) for lower frequencies.

Given the numerical results, apart from the differences in coincidence frequency and wave's speed (shown in table 3), the general behaviour is very similar. Given the fact that both materials are considered to be isotropic, it would be interesting to compare these results with real data.

Appendix C. Aluminium Plates

INSPECTION CERTIFICATE	No: 2487 Date: 3/1/2011	CERTIFIED SRAC-IQNet ISO 9001/2001 No. 10/4-2008	vimetco alro SLATINA

CUSTOMER : METALLSERVICE IN GOTHEBURG AB

CONTRACT/ORDER : 1963
BILL OF DELIVERY : 80092897
TRUCK/CONTAINER : TM 20 SCR/ TM 14 GUR

MATERIAL : ALUMINIUM PLATES
ALLOY : EN AW-5754 **TEMPER:** H111
DIMENSIONS (mm) : 70035634 - . 8X1020X2020
70035635 - . 10X1020X2020
. - .

ACCORDING TO : EN 485 - 515 - 573

MECHANICAL PROPERTIES **1 MPa = 1 N/mm2 = 0.145 ksi = 0.102 kgf/mm2**

	1 lbs = 0.4536 kg	Rm Mpa		Rp0.2 Mpa		Elong. % 50mm	Hardness HB
		min.	max.	min.	max.	min.	min.
	Specified values:	190	240	80		18	52
LOT / BATCH	CASE / NET WEIGHT kg	Measured values:					
70035634 . S10111131	82109 / 1164	213		121		35	54.6
70035635 . S11020133	82107 / 1034	209		157		29	59.1
. .							

CHEMICAL COMPOSITION %

BATCH		Si	Fe	Cu	Mn	Mg	Cr	Ni	Zn	Ti	Ga	V	Al
S10111131		0.29	0.16	0.025	0.24	2.77	0.015	0.005	0.022	0.015	0.01	0.019	REM.
S11020133		0.26	0.22	0.065	0.21	2.73	0.028	0.005	0.083	0.026	0.01	0.014	REM.
.													REM
Acc. Standard	Min.					2.6							REM.
	Max.	0.4	0.4	0.1	0.5	3.6	0.3	0.05	0.2	0.15	0.05	0.05	
	Remarks:	0.10 -0.6 Mn+Cr					Other- Each- Max.: 0.05			OthersTotal- Max.: 0.15			

REMARKS:

ACCORDING TO: EN 485-2:2008; EN 515:1993; EN 573-3:2009

We hereby certify that the material detailed hereon has been produced and tested according to the requirements of the relevant specification and/or order. Keep in dry conditions, without larges temperatures variations. The differences between metal and air must be maxim 11 degrees C.

According to **EN 10204:2004 3.1**

QUALITY CONTROL DEPT.

ALRO S.A. No.116, Pitesti Street Phone: +(40) 0249 435 117; 0249 432 956 alro@alro.ro
230048-Slatina-ROMANIA Fax: (40) 0249 411 487; 0249 415 992 www.alro.ro

cod f1/PO-051/Rev.1/2008

Appendix D. Leaky Lamb Waves - LLW

At very high frequencies, when the thickness of the elastic plate is much bigger than wavelength of the waves propagated inside it, the wave pack travelling inside the plate is the result of the addition of longitudinal waves, L- Waves, travelling parallel to the surface and shear waves, T- Waves according to Kuttruff, Heinrich [18]. The waveguide generated is called Lamb waves, provided that no stress is applied on the surfaces of the plate, in the situation in which point force is applied on one of the plate's surfaces those waves are called Leaky Lamb waves, LLW, given that an analysis of their propagation shows the frequencies at which the energy leaks to the adjacent media, in this case water.

The summation of T- Waves and L- Waves results in a wave pattern in which two different motions can be observed:

$$\frac{\partial^2 \emptyset}{\partial x_1^2} + \frac{\partial^2 \emptyset}{\partial x_3^2} = \frac{1}{C_L^2}\frac{\partial^2 \emptyset}{\partial t^2} \quad \text{L – Waves} \qquad (54)$$

$$\frac{\partial^2 \psi}{\partial x_1^2} + \frac{\partial^2 \psi}{\partial x_3^2} = \frac{1}{C_T^2}\frac{\partial^2 \psi}{\partial t^2} \quad \text{T – Waves} \qquad (55)$$

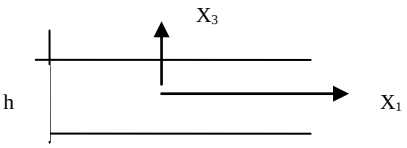

Figure 51. Coordinates system

$$\psi = \psi(x_3)e^{i(kx_1 - \omega t)} \qquad (56)$$

$$\phi = \phi(x_3)e^{i(kx_1 - \omega t)} \qquad (57)$$

Where

$\emptyset, \psi$ longitudinal and torsion displacement [m]

$x_1\ x_2\ x_3$ coordinate axis

t time [s]

c_L, c_T longitudinal (compressional) and transversal (shear) speed. Already explained in equation (1) and (2) respectively.

k wavenumber [m^{-1}] defined in equation (7)

ω angular frequency [rad/s] $\omega = 2\pi f$

The calculation of the waveguide phase speed can be carried out according to Snell's Law, considering the generation of travelling - standing waves in the axis $x_1\ x_3$ as shown in figure 51. The observance of the standing wave leads to the analysis of symmetrical – anti-symmetrical modes, therefore zeros – poles and from the examination of the poles the reflection to the adjacent media can be seen. Hence, the waveguide performs as follows:

$$\phi(x_3) = A_1 \sin(px_3) + A_2 \cos(px_3) \qquad (58)$$

$$\psi(x_3) = B_1 \sin(qx_3) + B_2 \cos(qx_3) \qquad (59)$$

A_1, A_2 amplitude of the standing wave travelling in x_3 axis

B_1, B_2 amplitude of the standing wave travelling in x_3 axis

The previous equations (58) – (59) contain terms with sinusoidal – cosines functions which represents symmetrical and antisymetrical displacements respect to the plate's the midplane.

Given the existence of cosines – sinus, the wave can be split in behaviours: symmetrical displacement reference to the mid plane (cosines) and anti- symmetrical. This fact yields to the shape of guided wave modes, which are independent and show response in frequency. As it is going to be shown later, the knowledge of the bulk - phase velocities is crucial to analyse the modal response and therefore the energy reflection. Note that for the study of the phase velocity in the water shear waves cannot be propagated; only L-waves can be emitted towards the fluid.

In the following calculations, incident angle perpendicular to the elastic layer has been studied and knowing bulk velocity in the fluid, the phase speed is calculated following Snell's Law.

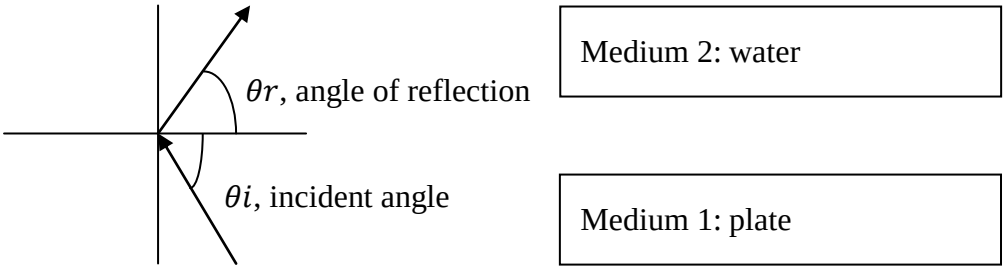

Figure 52. Snell's Law

If considered an incident angle of 90^0

$$\frac{cphase}{\sin\theta i} = \frac{cfluid}{\sin\theta r} \quad \rightarrow \quad cphase = \frac{cfluid}{\sin\theta r} \qquad (60)$$

Bulk velocity is the average fluid velocity, consider no dispersive c = 1500 m/s.

Hence, by following the next approximations, the energy reflection at the elastic layer (towards water) can be observed

The target situation in this project is to enhance radiation. Hence, there is energy leak and reflection R has minimum value, *Ultrasonics: fundamentals and applications* [18].

- $C_{phase} > C_{fluid}$ → Those frequencies should be avoided if the goal is to enhance radiation.

$$R = \frac{AS - Y^2}{(S+iY)(A-iY)} \qquad (61)$$

$$A = \frac{(q^2-1)^2}{q}\tan\left(kp\frac{d}{2}\right) + 4p\ \tan\left(kp\frac{d}{2}\right) \qquad (62)$$

$$S = \frac{(q^2-1)^2}{q}\cot\left(kp\frac{d}{2}\right) + 4p\ \cot\left(kp\frac{d}{2}\right) \qquad (63)$$

$$p^2 = (c/c_L)^2 - 1$$
$$q^2 = (c/c_T)^2 - 1$$

Where:

A, S anti-symmetric and symmetric modes correspondingly.

R energy reflection.

c_L, c_T, c are L- Wave, T- Wave and fluid bulk velocity. Equations (1) and (2).

Whereas fluid loading can be calculated as:

$$Y = \frac{\rho}{\rho_s}\left(\frac{c}{c_T}\right)^4 \frac{p}{qm} \qquad (64)$$

$$m = \left(\frac{c_{phase}}{c}\right)^2 - 1 \qquad (65)$$

Analysis, incident angles:

Case	1	2	3	4	5
Incident angle	90	112.5	135	157.5	180
c_{phase}	5436	5883	7687	1.42e4	4.43e19

Table 21. c_{phase} depending on the incident angle.

When the wave hits the elastic layer perpendicularly and the reflected wave not deviated, θr = 90º, the energy transmitted towards the water travels with a velocity equal to the bulk velocity, thus all the energy is transmitted. Besides, for small reflected angles close to 0º, the phase velocity tends to infinity.

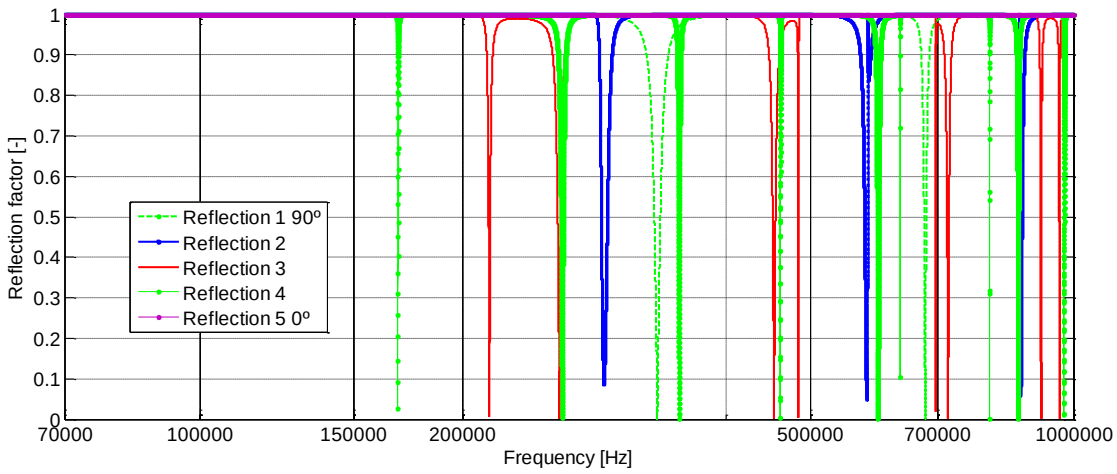

Figure 53. Reflection factor.

As it can be seen in the previous figure, this approach considers first order effects from frequencies around 170 kHz onwards. Thus, out of the frequency range of scope in this thesis.